

Dynamic Modelling of CO<sub>2</sub> Sequestration  
In the  
Harvey Area

A Report by ODIN Reservoir Consultants

For

Department of Mines and Petroleum

DMP/2016/5



July 2016

<b>LIST OF FIGURES</b> .....	<b>3</b>
<b>LIST OF TABLES</b> .....	<b>4</b>
<b>DECLARATION</b> .....	<b>5</b>
<b>NOTE:</b> .....	<b>5</b>
<b>1. EXECUTIVE SUMMARY</b> .....	<b>6</b>
<b>2. INTRODUCTION</b> .....	<b>7</b>
<b>3. INPUT DATA</b> .....	<b>8</b>
3.1 TEMPERATURE REGIME .....	8
3.2 PRESSURE REGIME .....	9
3.3 FLUID FLOW PROPERTIES.....	10
3.3.1 CO <sub>2</sub> relative Permeability and Trapped Gas Saturation (Sg <sub>T</sub> ) .....	11
3.3.1.1 Trapped Gas Saturation (Sg <sub>T</sub> ).....	11
3.4 WATER RELATIVE PERMEABILITY.....	13
3.4.1 CO <sub>2</sub> Relative Permeability .....	14
3.5 BRINE SALINITY .....	14
3.6 GEOMECHANICS .....	15
3.7 GEOLOGICAL MODEL .....	19
<b>4. UPSCALING</b> .....	<b>20</b>
4.1 DESCRIPTION OF THE SECTOR MODELS.....	21
4.1.1 Model Run Parameters .....	22
4.2 MODEL RESULTS.....	25
4.2.1 Yalgorup.....	25
4.2.2 Wonnerup .....	26
<b>5. INJECTIVITY STUDIES</b> .....	<b>29</b>
5.1 REFERENCE CASE.....	29
5.2 IMPACT OF RESERVOIR UNCERTAINTIES .....	30
<b>6. MODELLING OF THE CO<sub>2</sub> PLUME</b> .....	<b>34</b>
6.1 SIMULATOR SELECTION .....	34
6.2 MODEL DESCRIPTION .....	34
6.3 INITIALISATION PARAMETERS.....	36
6.4 PVT MODEL.....	37
6.5 AQUIFER EXTENT .....	37
6.6 RESERVOIR PROPERTIES.....	38
6.7 CONCEPTUAL DEVELOPMENT PLAN – REFERENCE CASE.....	40
6.7.1 Reference Case Definition .....	40
6.7.2 Results .....	41
6.8 IMPACT OF RESERVOIR UNCERTAINTIES ON THE MOVEMENT OF THE CO <sub>2</sub> PLUME .....	45
6.8.1 Case 1 – High Vertical Permeability (“Holey Faults”) .....	45
6.8.2 Case 2 – High Gas Relative Permeability (krg=0.23) .....	47
6.8.3 Case 3 – Low Trapped Gas Saturation (Sg <sub>T</sub> =0.10) .....	49
6.8.4 Case 4 - High Permeability Case.....	50
6.8.5 Case 5 – High kv/kh (Vertical to Horizontal Permeability Ratio).....	52
6.8.6 Case 6 – Deterministic Scenario .....	53
6.8.7 Case 7 – Faults transmissibility multiplied by 0.1 .....	56
6.8.8 Case 8 – Low CO <sub>2</sub> Solubility.....	57
<b>7. STRESS SCENARIOS</b> .....	<b>60</b>
7.1 CASE 9 - HIGH RATE.....	60
7.2 CASE 10 – LOW SOLUBILITY AND LOW TRAPPED GAS SATURATION .....	62
<b>8. FURTHER WORK</b> .....	<b>64</b>

## 9. REFERENCES ..... 65

### List of Figures

Figure 1 Location Map of the Harvey Area showing the Area of Interest.....	7
Figure 2 Temperature Measurements for the Harvey wells .....	8
Figure 3 Pressure data from RCI tool run in Harvey-1 and Harvey-4 .....	9
Figure 4 Steady-state imbibition data (Sample 20) – Harvey-3 .....	12
Figure 5 Water Relative Permeability Data (Harvey-1 and Harvey-3) .....	13
Figure 6 Drainage and Imbibition Water Relative Permeability (Sample 20 Harvey-3) .....	14
Figure 7 Geomechanical Model A - Yalgorup .....	16
Figure 8 Geomechanical Model B - Yalgorup .....	17
Figure 9 Geomechanical Model C – Yalgorup .....	17
Figure 10 Geomechanical Model A - Wonnerup .....	18
Figure 11 Geomechanical Model B - Wonnerup .....	18
Figure 12 Geomechanical Model C - Wonnerup .....	19
Figure 13 View of the Petrel Model of the Area of Interest in the Harvey Area .....	20
Figure 14 View of the Petrel Model showing the area selected for the Sector model.....	21
Figure 15 Sector Model of the Yalgorup and Wonnerup .....	23
Figure 16 Sector Model Showing Pore Volume Multipliers .....	24
Figure 17 Reference Case Relative Permeability Curves .....	24
Figure 18 Bottom hole pressure Response - Yalgorup Model .....	26
Figure 19 Gas Saturation Distribution – Yalgorup .....	26
Figure 20 Bottom hole pressure Response - Wonnerup Model .....	27
Figure 21 Gas Saturation Distribution – Wonnerup (Comparison of 1 and 2 m models)...	27
Figure 22 Gas Saturation Distribution – Wonnerup (Comparison of 1 and 4 m models)...	28
Figure 23 Reference Case Model – Injection Performance (Single Well Model).....	30
Figure 24 Tornado Chart Showing Impact of Reservoir Uncertainties on Injectivity .....	32
Figure 25 Probability Distribution of Injectivity Over 30 Years .....	33
Figure 26 Coarse Scale Model Showing Porosity Distribution .....	35
Figure 27 Comparison of Permeability Distribution - Fine and Coarse Scale Models .....	36
Figure 28 Connected Body Analysis - Fine and Coarse Scale Models.....	36
Figure 29 Time Structure maps of the: a) top Yalgorup Member; b) top Wonnerup Member (After Reference 7).....	37
Figure 30 Modelling the Extent of the Wonnerup and Yalgorup Aquifers .....	38
Figure 31 X-Section through the Harvey Full Field Model – Horizontal Permeability .....	39
Figure 32 X-Section through the Harvey Full Field Model – Vertical Permeability .....	39
Figure 33 X-Section through the Harvey Full Field Model – Porosity .....	40
Figure 34 Injection Performance – Reference Case .....	42
Figure 35 Bottom Hole Pressure Profile by Well During Injection – Reference Case.....	43
Figure 36 Top View – Reference Case CO <sub>2</sub> Distribution at end of Injection Period .....	43
Figure 37 Top View – Reference Case CO <sub>2</sub> Distribution 1000 years after injection .....	44
Figure 38 Reference Case – X-Section through HI-2 and HI-6.....	44
Figure 39 X-Section (I=35) through the model showing high permeability conduits .....	46
Figure 40 Top View – CO <sub>2</sub> Distribution (Comparison of Reference Case and Case 1) .....	46
Figure 41 X-Section View – CO <sub>2</sub> Distribution (Comparison of Reference Case and Case 1).....	47
Figure 42 Gas Relative Permeability (Comparison of Reference Case and Case 2) .....	48
Figure 43 Top View – CO <sub>2</sub> Distribution (Comparison of Reference Case and Case 2) .....	48
Figure 44 X-Section View – CO <sub>2</sub> Distribution (Case 2) .....	49
Figure 45 Top View – CO <sub>2</sub> Distribution (Comparison of Reference Case and Case 3) .....	50
Figure 46 X-Section View – CO <sub>2</sub> Distribution (Case 3) .....	50
Figure 47 Top View – CO <sub>2</sub> Distribution (Comparison of Reference Case and Case 4) .....	51
Figure 48 X-Section View – CO <sub>2</sub> Distribution (Case 4) .....	51
Figure 49 Top View – CO <sub>2</sub> Distribution (Comparison of Reference Case and Case 5) .....	52
Figure 50 X-Section View – CO <sub>2</sub> Distribution (Case 5) .....	53
Figure 51 Harvey-1 – Gamma ray and interpreted porosity log. ....	54

Figure 52 Top View – CO <sub>2</sub> Distribution (Comparison of Reference Case and Case 6) .....	55
Figure 53 X-Section View – CO <sub>2</sub> Distribution (Case 6) .....	55
Figure 54 Top View – CO <sub>2</sub> Distribution (Comparison of Reference Case and Case 7) .....	56
Figure 55 X-Section View – CO <sub>2</sub> Distribution (Case 7) .....	57
Figure 56 CO <sub>2</sub> Solubility in Brine (500 years after Cessation of Injection) .....	58
Figure 57 Top View – CO <sub>2</sub> Distribution (Comparison of Reference Case and Case 8) .....	58
Figure 58 X-Section View – CO <sub>2</sub> Distribution (Case 8) .....	59
Figure 59 Injection Performance –Case 9 .....	61
Figure 60 Bottom Hole Pressure Profile by Well During Injection – High Rate Case .....	61
Figure 61 Top View - CO <sub>2</sub> Distribution (Reference Case and Case 9) .....	62
Figure 62 X-Section View – CO <sub>2</sub> Distribution (Case 9) .....	62
Figure 63 Top View - CO <sub>2</sub> Distribution (Reference Case and Case 10) .....	63
Figure 64 X-Section View – CO <sub>2</sub> Distribution (Case 10) .....	63

### List of Tables

Table 1 Special Core Analysis sample Distribution (Harvey-1, -3 and -4) .....	10
Table 2 Primary Drainage and Primary Imbibition (CSIRO data – Reference 1) .....	11
Table 3 Water Displacing CO <sub>2</sub> - Sample 20 (Harvey-3) .....	12
Table 4 Brine Samples from Harvey.....	15
Table 5 Impact of Reservoir Uncertainties on Injectivity in the Wonneerup .....	31
Table 6 Range of Gas injected – Combined Uncertainties .....	33
Table 7 Material Balance Accounting (1000 Years after Injection) .....	45
Table 8 Case Summary – Full Field Model of the Harvey Area .....	45
Table 9 Summary Table for Stress Scenarios.....	60

## **Declaration**

*ODIN Reservoir Consultants has been commissioned to undertake to provide a reservoir modelling study for the South West Hub CO<sub>2</sub> Sequestration Project on behalf of The Department of Minerals and Petroleum, (DMP)*

*The evaluation of Carbon Capture and Storage is subject to uncertainty because it involves judgments on many variables that cannot be precisely assessed, including CO<sub>2</sub> sequestration rates and capture, the costs associated with storing these volumes, sequestration gas distribution and potential impact of fiscal/regulatory changes.*

*The statements and opinions attributable to us are given in good faith and in the belief that such statements are neither false nor misleading. In carrying out our tasks, we have considered and relied upon information supplied by the DMP and available in the public domain. Whilst every effort has been made to verify data and resolve apparent inconsistencies, neither ODIN Reservoir Consultants nor its servants accept any liability for its accuracy, nor do we warrant that our enquiries have revealed all of the matters, which an extensive examination should disclose.*

*We believe our review and conclusions are sound but no warranty of accuracy or reliability is given to our conclusions.*

*Neither ODIN Reservoir Consultants nor its employees has any pecuniary interest or other interest in the assets evaluated other than to the extent of the professional fees receivable for the preparation of this report*

### **Note:**

*ODIN has conducted the attached independent technical evaluation with the following internationally recognised specialists:*

**David Lim** is a member of the Society of Petroleum Engineers (SPE). He has over 30 years of international reservoir engineering experience in Europe, North and South America, North and West Africa, Middle East, Asia and Australasia. David is an internationally recognised reservoir simulation and reservoir engineering expert and has specialist expertise in field development planning, reservoir engineering, reserves reviews and simulation. David has been the Reservoir Simulation and Reservoir Engineering Advisor to NOCs, major and independent operators in Australia and SE Asia. David has also chaired SPE committees and forums on reservoir simulation, well testing and field development planning.

## 1. EXECUTIVE SUMMARY

---

ODIN Reservoir Consultants has been commissioned by the Department of Mines and Petroleum (WA) to provide a multi-disciplinary group with sub-surface skill sets to:

- 1) Undertake an interpretation of the 3D seismic data;
- 2) provide support through reservoir model building and updating of the South West Hub Project in the southern Perth Basin; and
- 3) provide on-going technical support.

As an integral part of the above, ODIN Reservoir Consultants conducted reservoir simulation studies to assess the suitability of the Lesueur Sandstone in the Lower Lesueur Region of Western Australia as a potential carbon dioxide geological sequestration site..

The objective of the simulation study is to provide a suite of full field simulation models which cover a range of subsurface uncertainties that provides confidence that the CO<sub>2</sub> plume stays below 800 mTVDss and within the storage complex for 1000 years. The results of this study will enable a Go/No Go decision on additional data acquisition in the Harvey area.

The results of the modelling show that it could be feasible to inject 800,000 tpa of CO<sub>2</sub> over 30 years in the Yalgorup and Wonnerup formations in the Harvey area. Our modelling studies show that all of the injected CO<sub>2</sub> remains in the Wonnerup and that the main factors controlling CO<sub>2</sub> plume migration are trapped gas saturation and the solubility of CO<sub>2</sub> in brine. Uncertainties in end point relative permeability, vertical permeability or the fraction of high energy facies in the Wonnerup are a second order effect. The study also highlights the lack of SCAL, steady state trapped gas saturation in particular, and water salinity data from the Harvey area which can be used to further constrain the range of results from the simulation studies.

ODIN also recommends that detailed fine grid simulations be conducted to examine the impact of coarsening the grid in the lateral direction and also to calibrate the solubility of CO<sub>2</sub> in the coarse grid blocks.

## 2. INTRODUCTION

ODIN Reservoir Consultants has been commissioned by the Department of Mines and Petroleum (WA) to provide a multi-disciplinary group with sub-surface skill sets to:

1. Undertake an interpretation of the 3D seismic data;
2. provide support through reservoir model building and updating of the South West Hub Project in the southern Perth Basin; and
3. provide on-going technical support.

As an integral part of the above, ODIN Reservoir Consultants conducted reservoir simulation studies to assess the suitability of the Lesueur Sandstone in the Lower Lesueur Region of Western Australia as a potential carbon dioxide geological sequestration site capable of injecting 800,000 tonnes per annum of CO<sub>2</sub> and containing the CO<sub>2</sub> for at least 1000 years of injection ceases.. The location and area of interest of the study is shown in Figure 1.

The objective of the simulation study is to provide suite of full field simulation models which cover uncertainties and demonstrate plume profiles over 1,000 years and containment of the plume below 800 mTVDss and within the storage complex for 1000 years that will enable a Go/No Go decision on additional data acquisition.

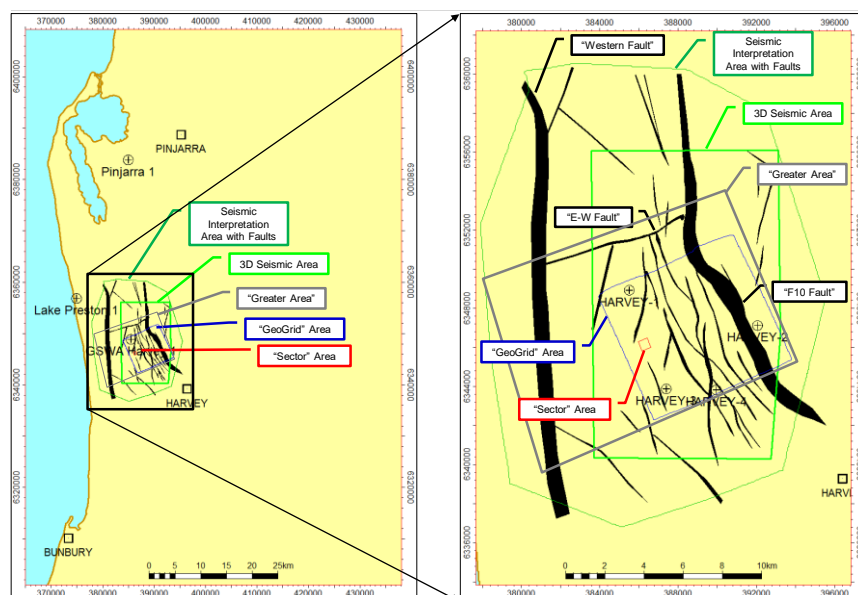


Figure 1 Location Map of the Harvey Area showing the Area of Interest

### 3. INPUT DATA

#### 3.1 Temperature Regime

Bottom hole temperatures were recorded on all the wireline logging runs in Harvey-1, -2, -3 and -4 (Figure 2). The maximum temperature recorded was nearly 76° C at a measured depth of about 2860m in Harvey-1. This represents a geothermal gradient of between 20-25 °C/km..

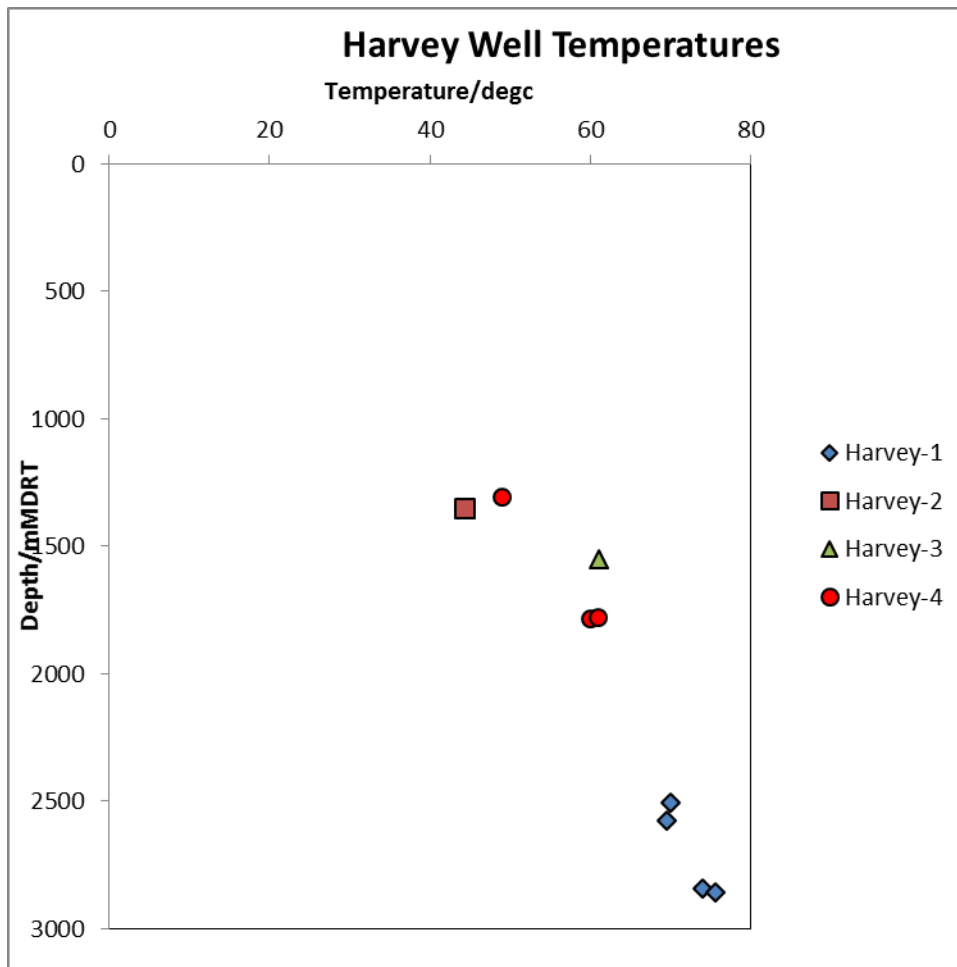


Figure 2 Temperature Measurements for the Harvey wells



### 3.2 Pressure Regime

Pressure measurements were made with the formation pressure sampling tools in Harvey-1 and Harvey-4 are summarized in Figure 3. The data are consistent with a normally pressured aquifer extending to surface.

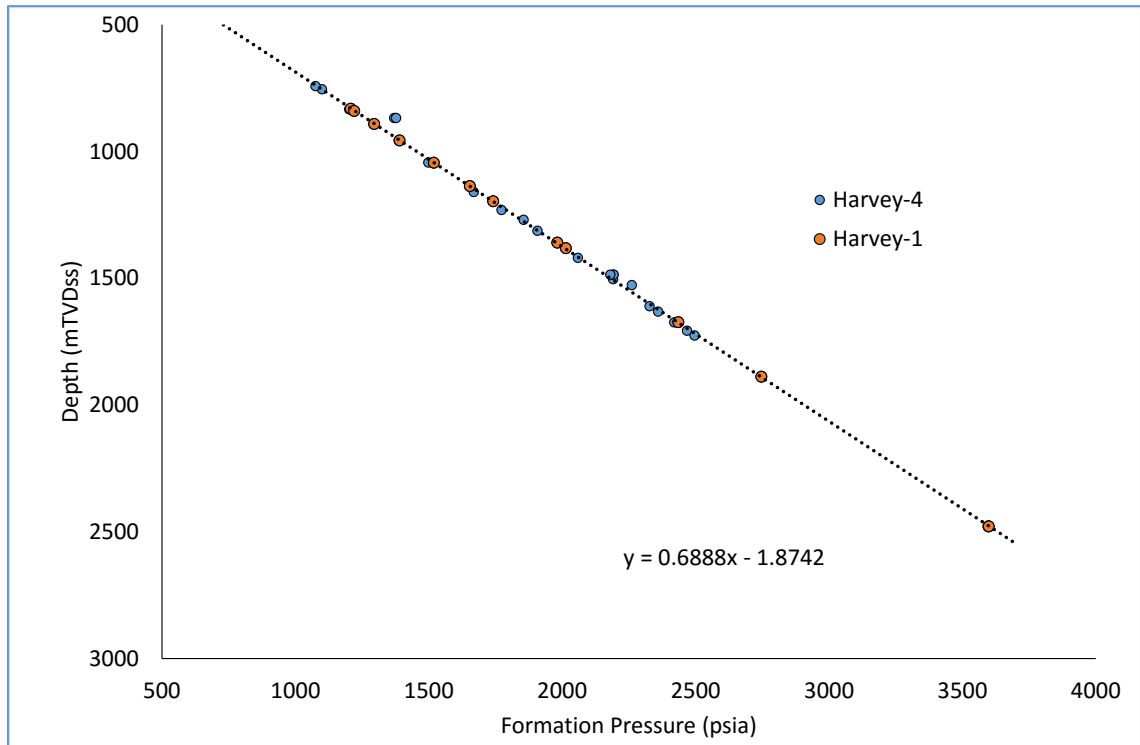


Figure 3 Pressure data from RCI tool run in Harvey-1 and Harvey-4

### 3.3 Fluid Flow Properties

Fluid flow properties on plugs from the Harvey cores were measured at in-situ reservoir conditions (Reference 1 and 2). End point relative permeability data were measured for eight samples from Harvey-3 (3 samples), Harvey-4 (2 samples) and Harvey-1 (3 samples). The plugs selected from the cores are from the two facies identified in the Wonnerup: Low Energy (L-E Fluvial) and High Energy (H-E Fluvial).

The experiments on the Harvey-1 samples were conducted by CSIRO and the experiments on the Harvey-3 and -4 samples were performed by Core Laboratories in Houston. All of the CSIRO experiments were conducted on plugs from the H-E fluvial.

Table 1 summarises the results of the core experiments.

The plugs representing the H-E Fluvial facies from Harvey-3 and -4 failed during the experiments. Steady state drainage and imbibition relative permeability curves were obtained from Sample 20 from the Harvey-3 core.

Facies	Well	Sample Number	Experiment	Sample Depth, meters	Porosity, fraction	Air Permeability, millidarcies	Initial Conditions			Terminal Conditions			Water Recovery, fraction	
							Water Saturation, fraction pore space	Specific		Water Saturation, fraction pore space	Effective Permeability to CO <sub>2</sub> , millidarcies	Relative Permeability to CO <sub>2</sub> * (k <sub>r</sub> /k <sub>w</sub> @SW=1), fraction		
								Permeability to Brine, millidarcies	Relative permeability to Water, (k <sub>r</sub> /k <sub>air</sub> )					
L-E Fluvial	H-3	20	SS	1429.0	0.22	22.0	1.00	4.24	0.19	0.49	0.79	0.19	0.51	0.51
L-E Fluvial	H-3	11	USS	1420.0	0.23	42.5	1.00	19.50	0.46	0.53	4.57	0.23	0.47	0.47
L-E Fluvial	H-4	8	USS	1799.0	0.17	67.7	1.00	18.00	0.27	0.42	2.63	0.15	0.58	0.58
H-E Fluvial	H-3	135	USS	1544.0	0.19	1130.0	1.00	530.00	0.47	0.57	58.00	0.11	0.43	0.43
H-E Fluvial	H-4	4	USS	1793.0	0.22	2720.0	1.00	2180.00	0.80	0.65	251.00	0.12	0.35	0.35
H-E Fluvial	H-1	206647	USS	1901.6	0.15	525.0	1.00	48.00	0.09	0.45	10.70	0.22	0.55	0.55
H-E Fluvial	H-1	206669	USS	2491.6	0.13	294.1	1.00	238.00	0.81	0.42	40.94	0.17	0.58	0.58
H-E Fluvial	H-1	206660	USS	1935.5	0.16	128.2	1.00	16.50	0.13	0.40	3.40	0.21	0.60	0.60

**Table 1 Special Core Analysis sample Distribution (Harvey-1, -3 and -4)**

### 3.3.1 CO<sub>2</sub> relative Permeability and Trapped Gas Saturation (Sg<sub>T</sub>)

#### 3.3.1.1 Trapped Gas Saturation (Sg<sub>T</sub>)

Unsteady state imbibition trapped gas saturations were measured on core plugs from Harvey-1. The trapped gas saturations on these core plugs ranged from 23%-43% (Table 2). Sg<sub>T</sub> from the unsteady state tests were not considered in this study as they were unreliable as the imbibition curves were unavailable and the end point gas relative permeability used to estimate the trapped gas saturation is unknown.

Curtin Samples H-1	Primary Drainage CO <sub>2</sub> Displacing Water	Primary Imbibition Water Displacing CO <sub>2</sub>	Primary Drainage CO <sub>2</sub> Displacing Water	Primary Imbibition Water Displacing CO <sub>2</sub>
	Final Sw	Final Sg	kr <sub>g</sub>	K <sub>rw</sub>
206647	45%	23%	0.22	0.35
206660	40%	43%	0.21	0.13
206669	42%	34%	0.17	0.10

**Table 2 Primary Drainage and Primary Imbibition (CSIRO data – Reference 1)**

Core Laboratories conducted drainage and imbibition relative permeability experiments on Sample 20 from Harvey-3 (Figure 4). Hysteresis in the CO<sub>2</sub> relative permeability data is evident and the reported Sg<sub>T</sub> of 0.265 (Table 3) from the steady state experiments. However, analysis of the data (Figure 4) shows that Sg<sub>T</sub> was estimated from CO<sub>2</sub> relative permeability >0.001. In our opinion that is too optimistic for CO<sub>2</sub> sequestration projects where project time scales are in the hundreds of years. We recommend that the trapped gas saturation, Sg<sub>T</sub>, should be estimated with lower CO<sub>2</sub> relative permeability. In our study, we have selected the Sg<sub>T</sub> of 0.19 at the minimum relative permeability of 0.00001.

In this study, the data from Core Laboratories was used to derive the trapped gas used in the modelling as the data from CSIRO is incomplete.

**WATER - CO<sub>2</sub> RELATIVE PERMEABILITY**

Steady State Method    Extracted State Samples  
 Net Confining Stress: 1700 psi    Temperature: 118°F

PETROLEUM SERVICES

Company: Department of Mines and Petroleum  
 Well: Harvey-3  
 Location: Australia

File: HOU-150878

Sample Number	Sample Depth, meters	Klinkenberg Permeability, millidarcies	Porosity, fraction	Initial Conditions		Terminal Conditions			CO <sub>2</sub> Recovery,	
				Water Saturation, fraction pore space	Effective Permeability to CO <sub>2</sub> , millidarcies	CO <sub>2</sub> Saturation, fraction pore space	Effective Permeability to Water, millidarcies	Relative Permeability to Water*, fraction	fraction pore space	fraction gas-in-place
20	1429.00	17.6	0.220	0.492	0.792	0.265	0.467	0.110	0.243	0.479

\* Relative to the Specific Permeability to Brine

**Table 3 Water Displacing CO<sub>2</sub> - Sample 20 (Harvey-3)**

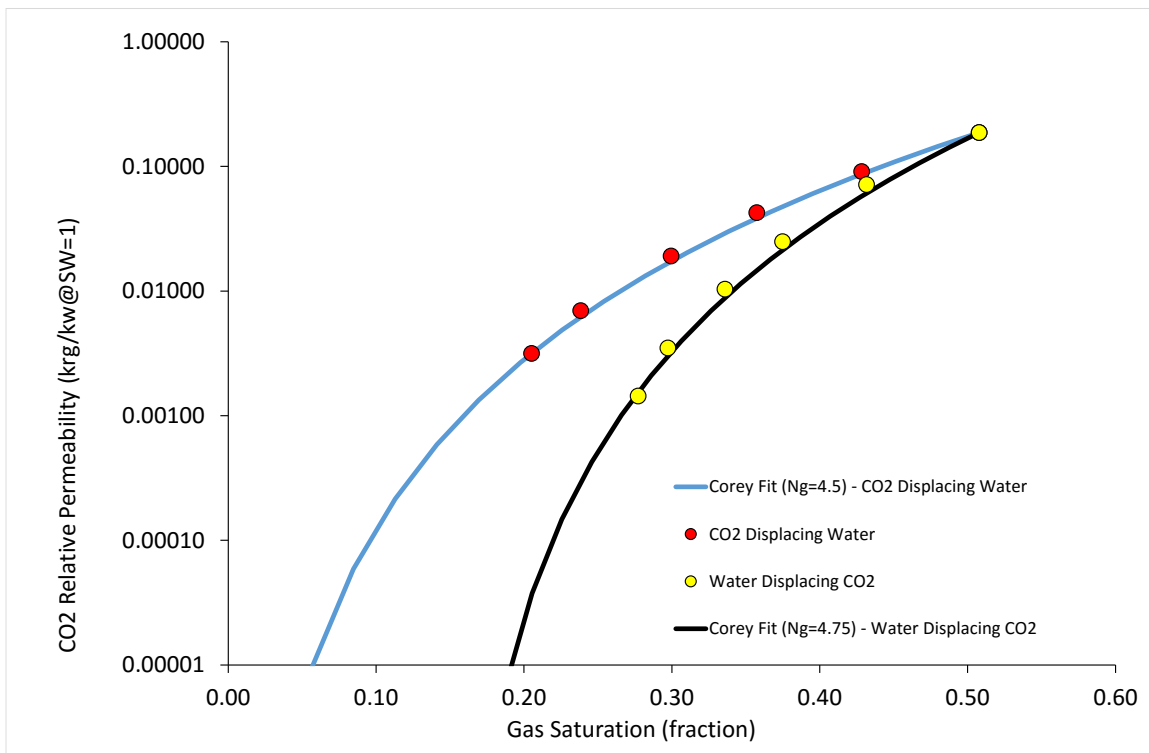


**Figure 4 Steady-state imbibition data (Sample 20) – Harvey-3**

### 3.4 Water Relative Permeability

Figure 5 shows the drainage and imbibition water relative permeability data from Harvey-1 and Harvey-3 plugs. No imbibition data from Harvey-1 were available. The data shows from the Harvey-1 plugs appear to be affected by small scale heterogeneities in the plugs and are likely to be unreliable.

Drainage and imbibition relative permeability data from Harvey-3 do not show any hysteresis and appear to be unaffected by small scale heterogeneities. The Harvey-3 data was very well fitted using a Corey exponent of 2.5 (Figure 6). The average water relative permeability measured on the plugs from the Harvey wells is, 0.37 @ SW=100%. This is unusual as one would expect the relative permeability to water at SW=100% to be 1. However, it is possible that the permeability to water was reduced due to fines movement.

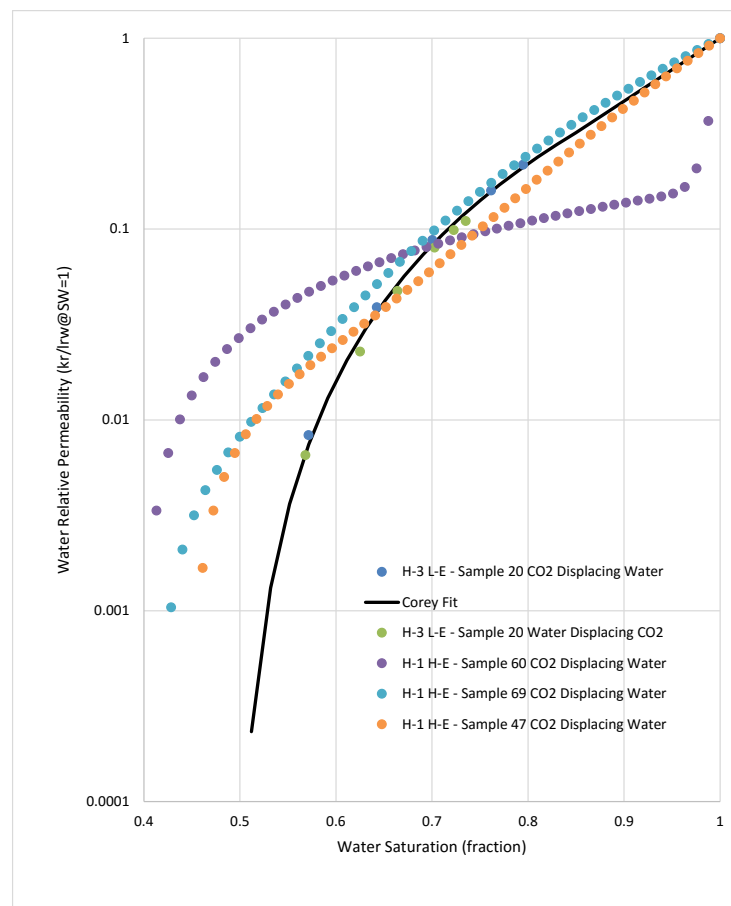


Figure 5 Water Relative Permeability Data (Harvey-1 and Harvey-3)

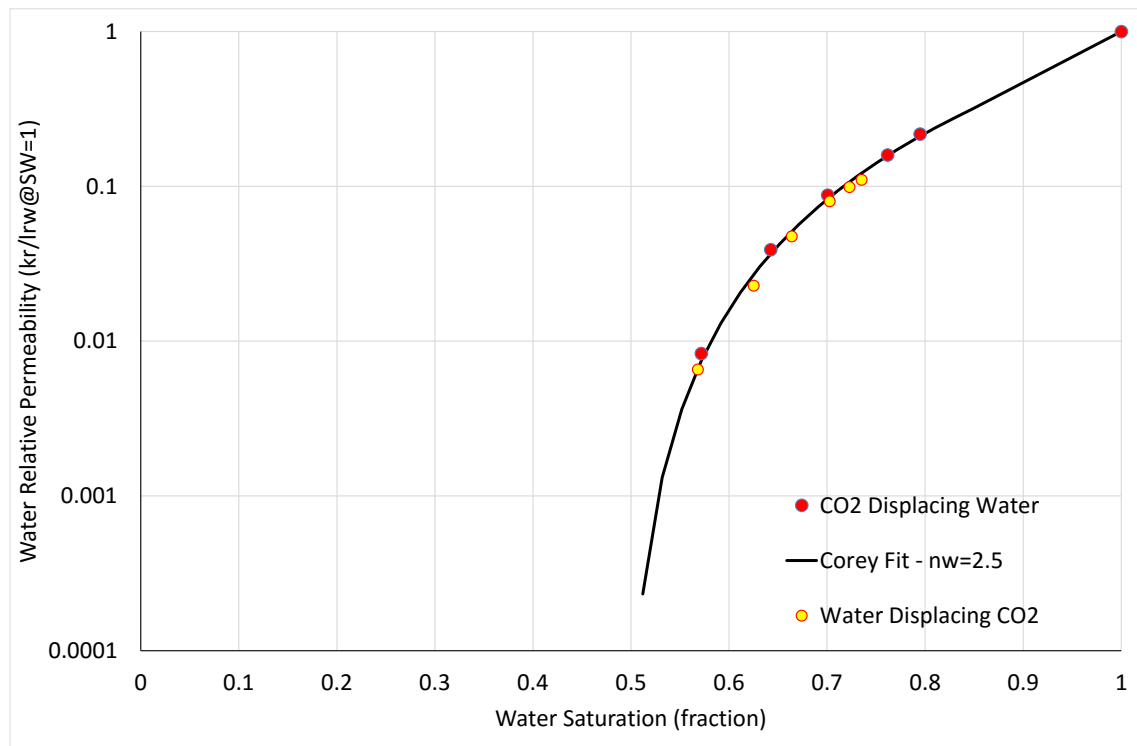


Figure 6 Drainage and Imbibition Water Relative Permeability (Sample 20 Harvey-3)

### 3.4.1 CO<sub>2</sub> Relative Permeability

Figure 4 show the CO<sub>2</sub> relative permeability data from both the unsteady state and steady state experiments. The drainage and imbibition relative permeability data were reasonably fitted with Corey exponents ranging from 4.5 to 4.75. Data from Harvey-1 were possibly affected by small scale heterogeneities in the plug (see Section 3.4). The imbibition CO<sub>2</sub> relative permeability data was fitted with a Corey exponent of 4.75. The average the end point CO<sub>2</sub> relative permeability from all of the plugs from the Harvey wells was 0.12 with an average SW<sub>min</sub> = 0.49.

### 3.5 Brine Salinity

Five water samples were retrieved from Harvey-3 and -4. All five samples were likely contaminated as suggested by elevated potassium and chloride figures (Reference 3). Both samples from Harvey-3 were heavily contaminated and are not reliable (Reference 5).

Three samples were retrieved from Harvey-4 and analysed by Core Laboratories (Reference 4). It was suggested that the contamination of Sample 1 from Harvey-4 was not as severe as the samples from Harvey-3. Core Laboratories used the sample from the Wonnerup as the basis of a synthetic “uncontaminated” brine composition for the Wonnerup.

Table 4 is a list of the water samples from Harvey. The synthetic sample from Core Laboratories was used in the full field simulation.

Well	Sample	TDS	NaCl Equivalent	Comments
		mg/L H <sub>2</sub> O	ppm	
Harvey-3	EP1511686-001	59900	51025	Contaminated sample from Wonnerup
Harvey-3	EP1511686-002	62600	58979	Contaminated sample from Wonnerup
Harvey-4	Sample 1 (1632.0 m)	45230	43650	RDT sample from Wonnerup
Harvey-4	Sample 3 (742.05 m)	70500	72046	RDT sample from Eneabba
Harvey-4	Sample 2 (1270.1 m)	156960	214782	RDT sample from Yalgorup
Synthetic	Core Lab	50001	46422	Synthetic Sample from Core Lab

**Table 4 Brine Samples from Harvey**

### 3.6 Geomechanics

A geomechanical study of the Harvey area was conducted by ODIN Reservoir Consultants (Reference 6) to assess the critical injection-induced pressures that could trigger shear failure along 3D seismic faults seen in the Harvey area. This assessment is necessary because if the faults situated in the Harvey CO<sub>2</sub> sequestration project area experience shear failure during injection operations, it is possible the faults could behave as conduits for unintended CO<sub>2</sub> migration. By identifying the critical injection-induced pressures tied to fault reactivation, this information can be used to control injection pressures and identify optimal well locations to minimise the risk of fault instabilities and subsequent unintended CO<sub>2</sub> migration.

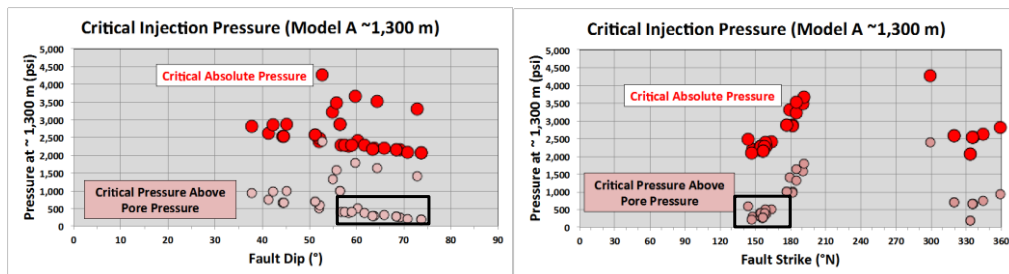
Due to large uncertainties in Shmin, three different geomechanical models of the Harvey area were used to calculate the critical fluid pressure, P<sub>critical</sub> (Figure 7 to Figure 12).

P<sub>critical</sub> corresponds to the instantaneous threshold pressure required to trigger shear failure along a fault or natural fracture. Because of the distance between the injection well and the fault in question, the resultant P<sub>critical</sub> is not the operational limits of injection pressures due to the pressure drop between the well and the fault as the pressure front advances.

$P_{critical}$  is the total applied pressure and a component of this total pressure is the reservoir pore pressure (PP). Therefore the incremental increase in injection-induced pressure would be ( $P_{critical} - PP$ ), or the critical pressure above PP.

In this study the injection pressure is constrained to 90% of the critical pressure above PP.

## Injection Pressures Model A – 1300 m Yalgorup

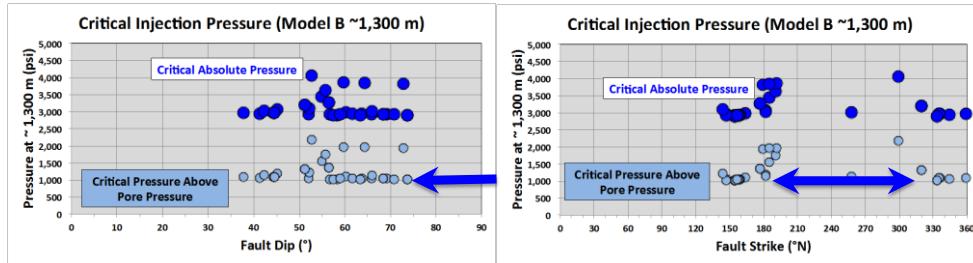


- Faults that may likely experience shear failure with instantaneous pulse of injection pressure of 500 psi or less are:
  - Dipping, 55-75°
  - Striking, 140°N-165°N and ~330°N

Figure 7 Geomechanical Model A - Yalgorup



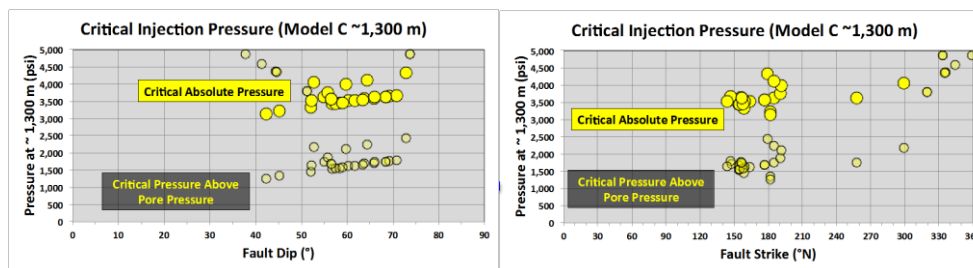
## Injection Pressures Model B – 1300 m Yalgorup



- In general, faults could support injection-induced pressures up to ~1,000 psi before experiencing shear failure.

Figure 8 Geomechanical Model B - Yalgorup

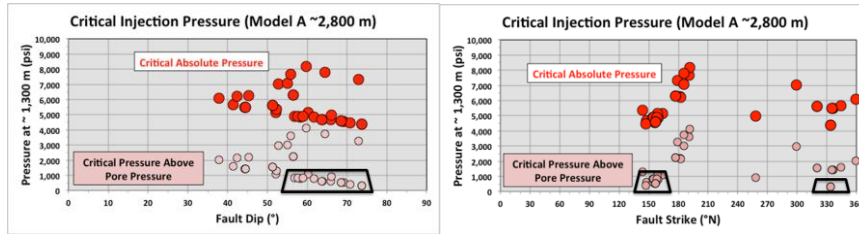
## Injection Pressures Model C – 1300 m Yalgorup



- In general, faults could support injection-induced pressures up to ~1,000 – 2000 psi before experiencing shear failure.

Figure 9 Geomechanical Model C – Yalgorup

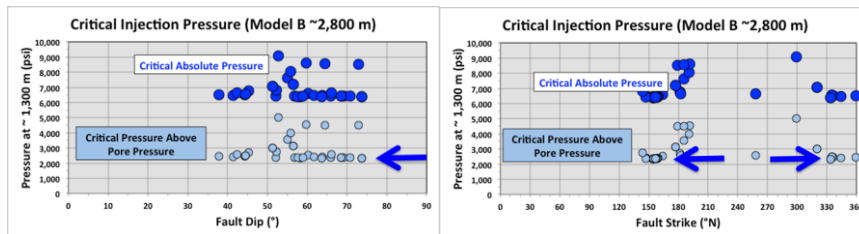
### Injection Pressures Model A – 2800 m Wonnerup



- Faults that may likely experience shear failure with instantaneous pulse of injection pressure of 500 psi or less are:
- Dipping, 55-75°
- Striking, 140°N-165°N and ~330°N

Figure 10 Geomechanical Model A - Wonnerup

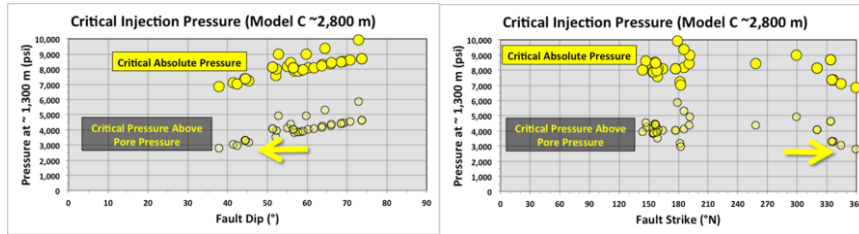
### Injection Pressures Model B – 2800 m Wonnerup



- In general, faults could support injection-induced pressures up to ~2100 psi before experiencing shear failure.

Figure 11 Geomechanical Model B - Wonnerup

## Injection Pressures Model C – 2800 m Wonnerup



- In general, faults could support injection-induced pressures up to ~2,700 psi before experiencing shear failure.

Figure 12 Geomechanical Model C - Wonnerup

### 3.7 Geological Model

Reservoir property and structural information for the Harvey model were imported directly from Petrel.

## 4. UPSCALING

The geological model of the Harvey area was constructed with cells of 25X25 metres and a vertical resolution of 1 metre to capture the vertical heterogeneity in the Yalgorup and Wonnerup. This resulted in a model with 166 million cells. It is impractical to simulate a model with that many cells (Figure 13). Grid sensitivity studies using sector models were conducted to investigate the level of vertical upscaling that can be applied and still retain the fluid flow properties. Vertical resolution is important to model the flow of gas in the vertical direction and improper upscaling can reduce the impact of baffles by combining cells with baffles with cells with high sand content which could result in cells which have no baffles to flow.

For the upscaling studies a 500 metre by 500 metre area of the full field model was extracted for simulations (Figure 14). The single well sector model is a subset of the Petrel model of the Harvey area and it is populated with reservoir properties which are consistent with the geological understanding of the Harvey area.

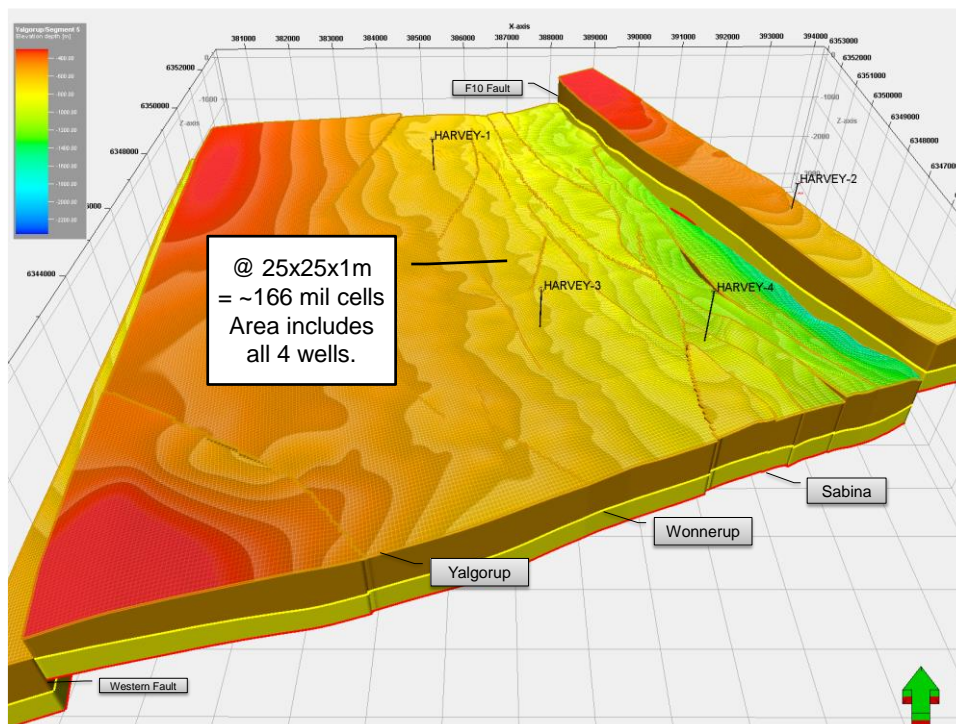


Figure 13 View of the Petrel Model of the Area of Interest in the Harvey Area

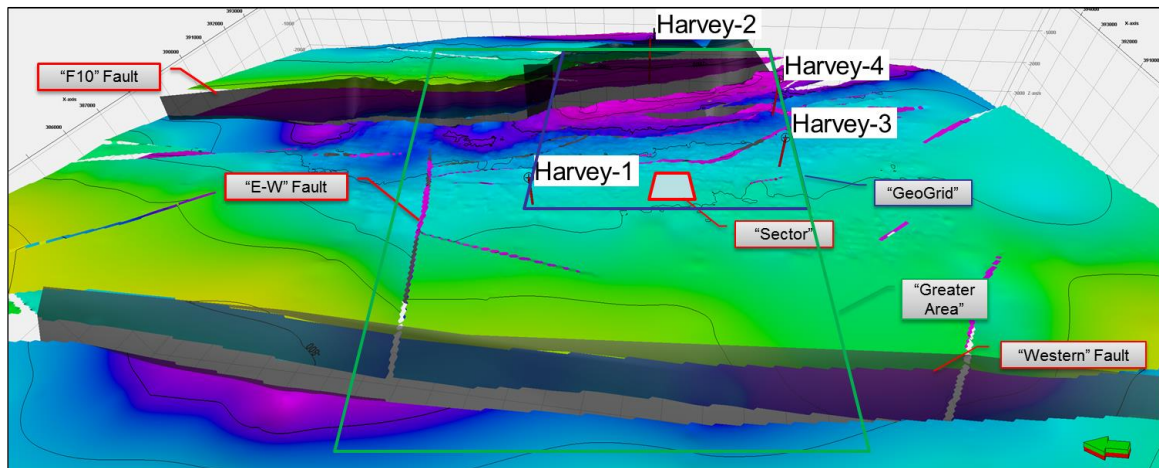


Figure 14 View of the Petrel Model showing the area selected for the Sector model.

#### 4.1 Description of the Sector Models

Three models were investigated:

- 1) 1 Metre in the vertical direction (Geological grid resolution)
  - The model dimensions are 20X20X2100.
  - Cell dimensions in the I- and J- direction are 25 metres
  - Yalgorup - Layers 1 to 700
  - Wonnerup- Layers 701 to 2100
  
- 2) 2 Metres in the vertical direction
  - The model dimensions are 20X20X1050.
  - Cell dimensions in the I- and J- direction are 25 metres
  - Yalgorup - Layers 1 to 350
  - Wonnerup- Layers 351 to 1050
  
- 3) 4 Metres in the vertical direction
  - The model dimensions are 20X20X525
  - Cell dimensions in the I- and J- direction are 25 metres
  - Yalgorup - Layers 1 to 175
  - Wonnerup- Layers 176 to 525

### 4.1.1 Model Run Parameters

The following parameters were used to initialise the sector model and constrain the runs.

- 1) Flow based upscaling in the Petrel model was used to upscale the cells in the vertical direction.
- 2) For expediency, a Black Oil model was used for simulations and the Yalgorup and Wonnerup reservoirs were run separately.
- 3) Dry gas PVT tables used in the simulation were generated with industry standard correlations with gas specific gravity of 0.75.
- 4) Relative Permeability (Figure 17).
  - a.  $K_{rw} @ (S_w=1) = 0.37$
  - b.  $K_{rg} @ (S_{wmin}=0.49) = 0.12$
  - c. Corey exponents
  - d.  $N_w = 4.0$
  - e.  $N_g = 4.5$
- 5) The model was initialised as a fully water saturated model at an initial pressure of 179 bars at a datum depth of 1801 metres.
- 6) A dry gas injector was located at I=10 and J=10 and dry gas was injected into the model. Figure 15 shows the sector model.
- 7) The injection rate was constrained to a maximum of 457,000 m<sup>3</sup>/d ( $\approx$  300,000 tpa).
- 8) The injection bottom hole pressure was constrained to Pore Pressure + 0.9\*69 bars (Geomechanics Model B).
- 9) Gas was injected into the models for 30 years.
- 10) In the Yalgorup model, the well was completed over the bottom 148 metres and in the Wonnerup model, the well was completed over the bottom 200 metres.

Pore volume multipliers were used to modify the edge cells of the sector model to match the aquifer surrounding the area defined by the sector (Figure 16). Without the pore volume multipliers the injection of the gas into the model would result in significant increase in reservoir pressure which would lead to the injection bottom hole constraint being violated.

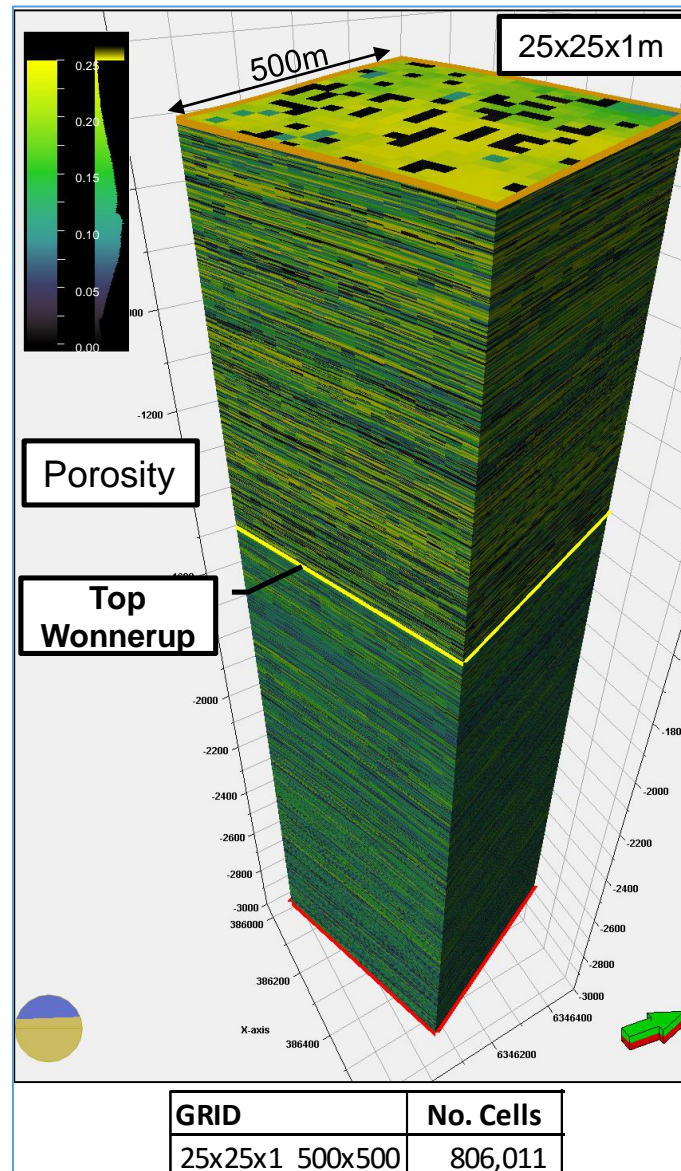
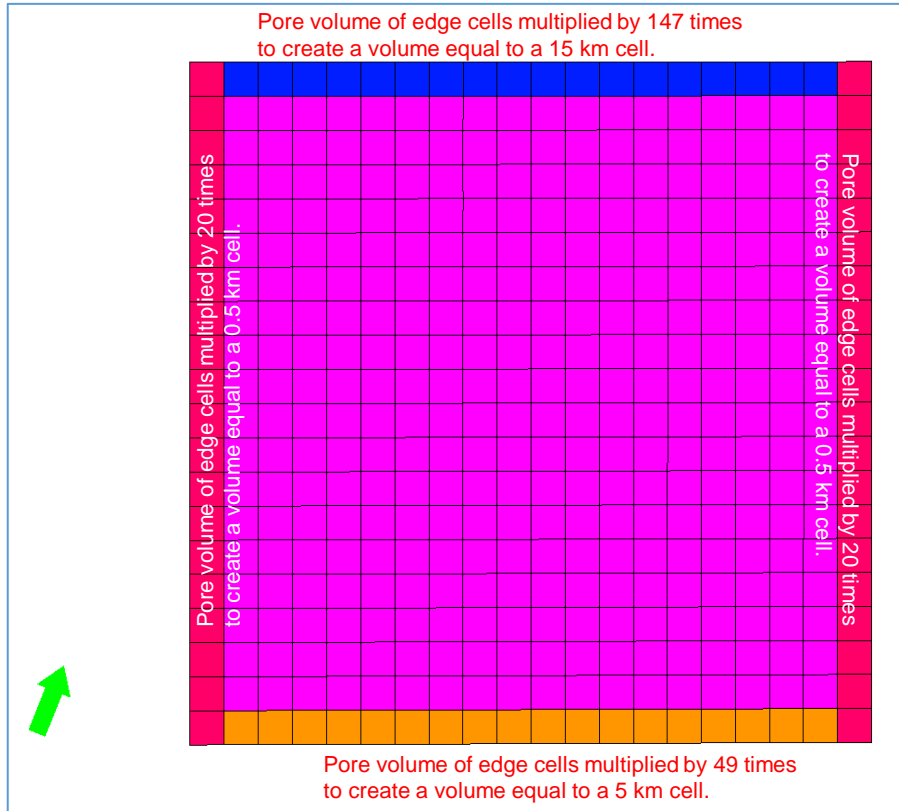
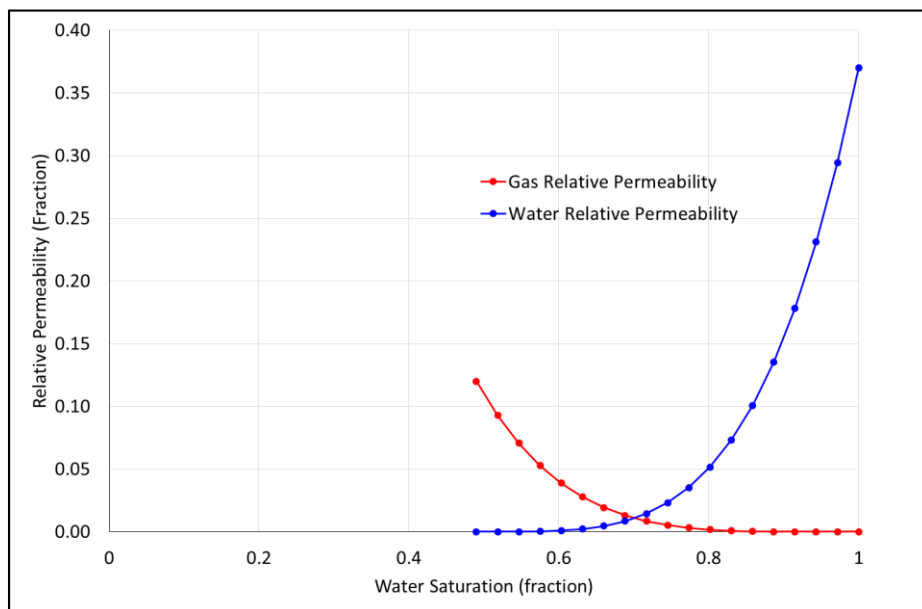


Figure 15 Sector Model of the Yalgorup and Wonnerup



**Figure 16 Sector Model Showing Pore Volume Multipliers**



**Figure 17 Reference Case Relative Permeability Curves**

Two criteria were used to evaluate the success of the upscaling:



- The bottom hole pressure during the injection should be almost identical for the same injection rate. This would demonstrate that the vertical connectivity is the same for the different grids.
- The saturation profiles in the models should be almost identical.

## 4.2 Model Results

### 4.2.1 Yalgorup

Figure 18 compares the bottom hole pressure response between the 1 metre (geological scale) model and the model with the vertical resolution of 2 metres. The results show that the BHP response is different in the two models. The lower injection pressures observed in the 2 metre model indicates that it is more connected compared to the 1 metre model. This indicates that some of the vertical baffles to flow have been smoothed out.

Figure 19 compares the gas saturation distribution in the model with 1 metre vertical resolution and the model with 2 metre vertical resolution. Gas saturation distribution in the 1 and 2 metre models at the end of run is quite different between the two models. Gas has migrated farther up the column in the 2 metre model compared to the 1 metre model. This indicates that the baffles to flow in the 1 metre model were “smoothed” out.

The results of the upscaling runs with the Yalgorup model indicates that vertical upscaling is not suitable for this sand.

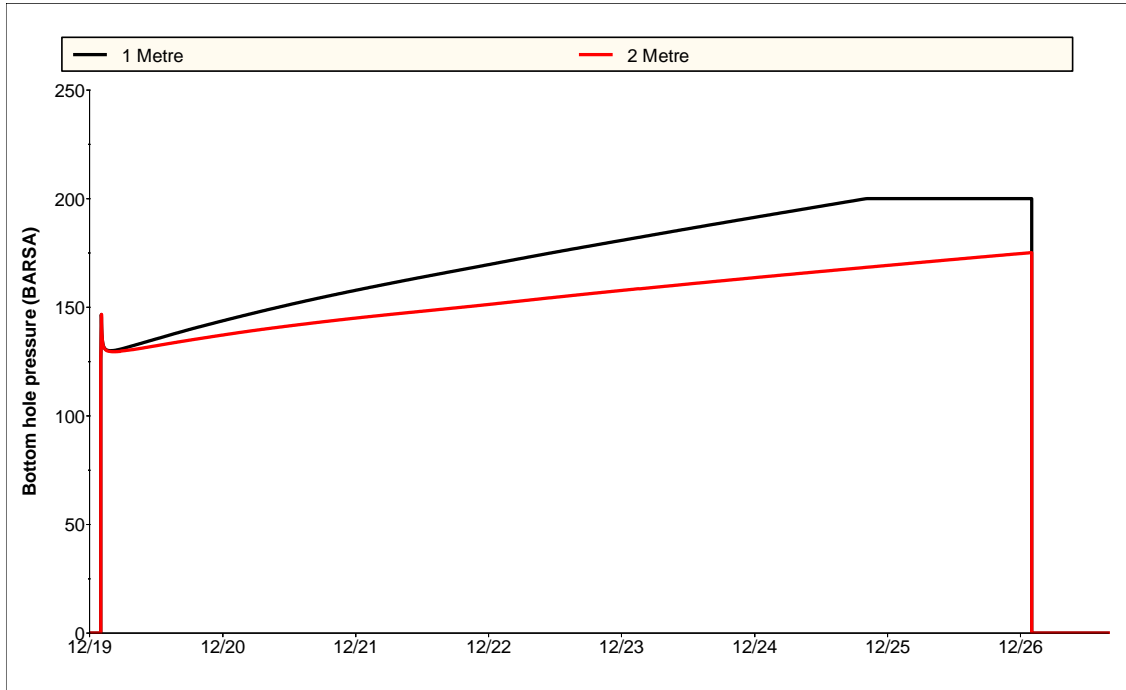


Figure 18 Bottom hole pressure Response - Yalgorup Model

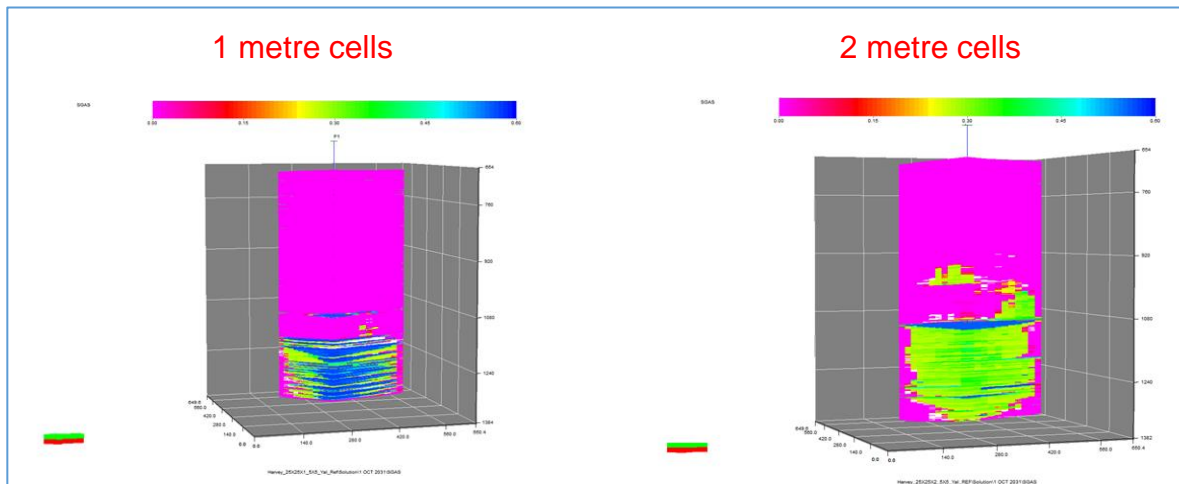


Figure 19 Gas Saturation Distribution – Yalgorup

#### 4.2.2 Wonnerup

Figure 20 shows that there is no material difference in the bottom hole pressure response for the Wonnerup models with 1, 2 and 4 metre vertical resolution. Figure 21 and Figure 22 shows that the gas saturation in the model with the 1 metre vertical resolution is similar

to the models with 2- and 4-metre vertical resolutions. These results indicate that the Wonnerup sands can be upscaled successfully to vertical resolution of 4 metres.

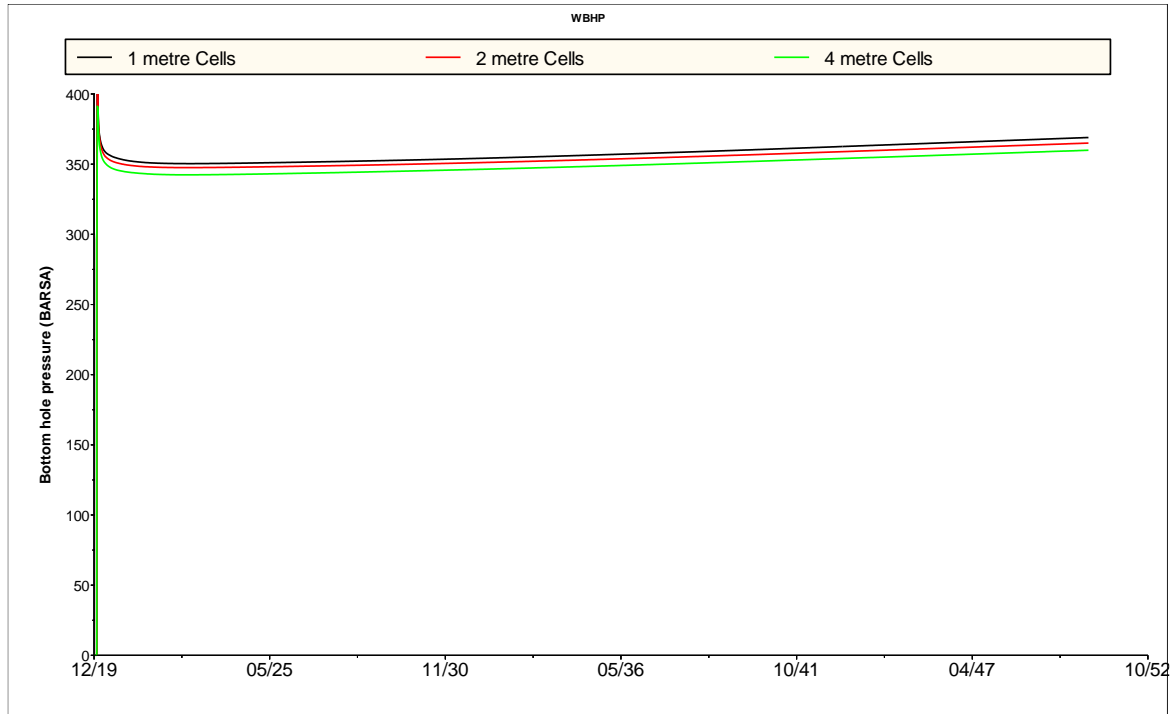


Figure 20 Bottom hole pressure Response - Wonnerup Model

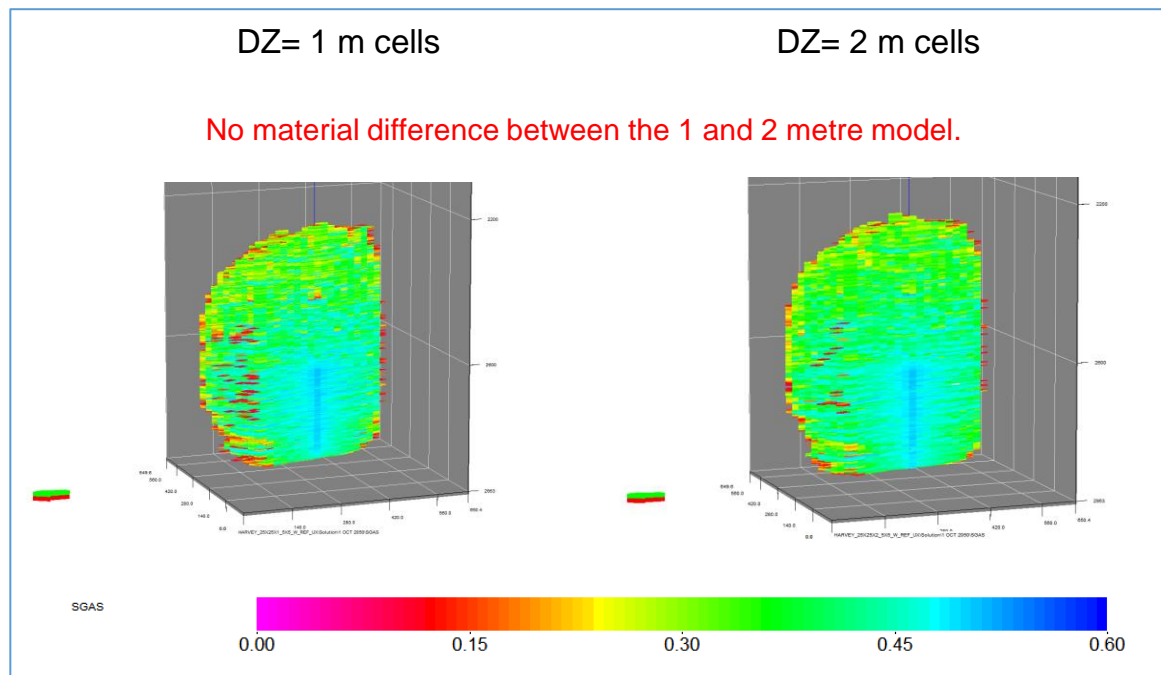
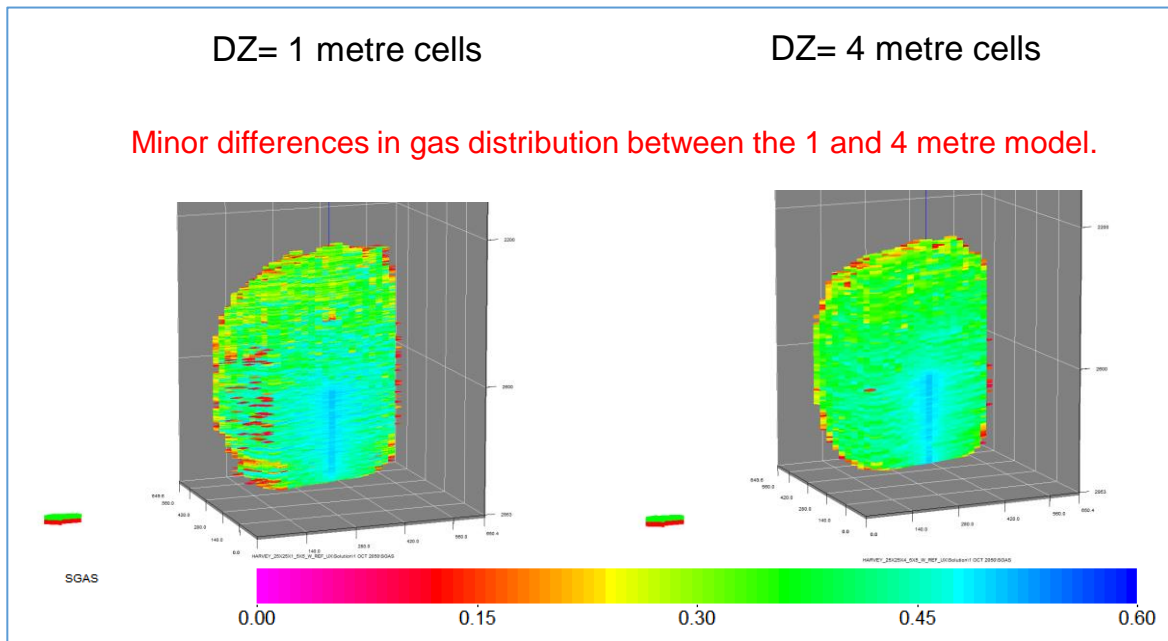


Figure 21 Gas Saturation Distribution – Wonnerup (Comparison of 1 and 2 m models)



**Figure 22 Gas Saturation Distribution – Wonnerup (Comparison of 1 and 4 m models)**

## 5. INJECTIVITY STUDIES

---

This phase of the dynamic modelling was conducted using the Wonnerup model with a vertical resolution of 4 metres. The objective of the study is to obtain probabilistic distribution of injection rates in the Wonnerup at a notional injection capacity of 3 -10 million tonnes per annum per well. As a guide ODIN is using a conceptual scenario of a project with 9-10 wells.

### 5.1 Reference Case

The Reference Case is defined below:

- Bottom hole pressure constraint = 360 bars @ 2948 m [Pore Pressure + 0.9\*69 bar]<sup>i</sup>
- Average kv/kh = 0.75 derived from Petrel model
- No damage skin.
- Well is completed in the bottom 250 metres for kh=20330 mD-m.
- Arbitrary start date of 1/1/2020

The results of the Reference Case model (Figure 23) shows that some 700 tonnes/day of gas could be injected into a well in the Wonnerup and that about 6.9 million tonnes can be injected over 30 years. Figure 23 shows injectivity declining as a function of time as the reservoir pressure increases due to the injection of gas.

---

<sup>i</sup> As there is significant uncertainty in the geomechanical model that is applicable in the Harvey area. A conservative injection pressure constraint was used. In this study, the injection pressures were constrained by Model B of the Yalgorup.

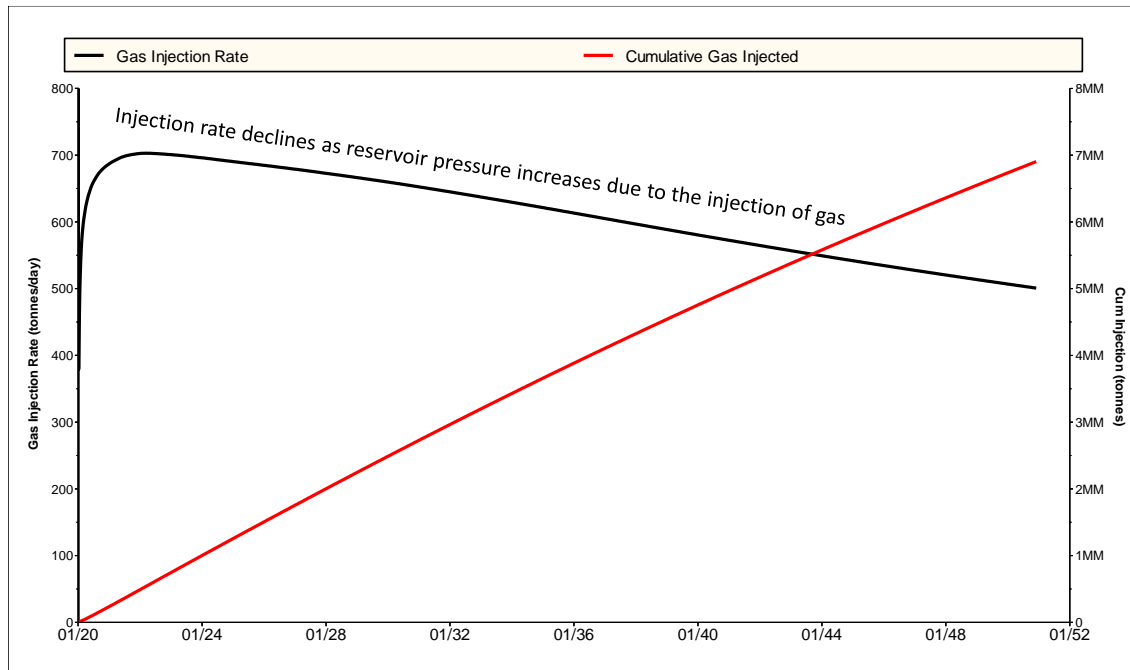


Figure 23 Reference Case Model – Injection Performance (Single Well Model)

## 5.2 Impact of Reservoir Uncertainties

The impact of reservoir uncertainties on injectivity in the Wonnerup was investigated by modifying the parameters of the Reference Case model. Listed below are the reservoir parameters investigated and the ranges of these parameters investigated.

- Permeability
  - Low Case – Reference Case permeability \* 0.7
  - High Case - Reference Case permeability \* 1.4
- Gas Relative Permeability
  - Low -  $k_{rg}=0.04$
  - High –  $k_{rg}=0.23$
- Water Relative Permeability
  - Low -  $k_{rw}=0.07$
  - High –  $k_{rg}=0.8$
- Low Kv/kh ratio – average  $k_v/k_h=0.31$

- Injection BHP Constraint (Pore Pressure + 0.9\*Critical Pressure)
  - Low – Model A (Critical pressure of 500 psi)
  - High - Model C (Critical pressure of 12500 psi)
  
- Model Volume (i.e. Small compartment)
  - Low Case – Northern and Southern cells reduced to 5 km. Edge cells in the East and West reduced to 0.25 km.

The results of the simulations are summarised in Table 5. A tornado chart of simulation results (Figure 24) show that gas relative permeability, bottom hole pressure constraint, the volume of the compartment and water relative permeability are the reservoir uncertainties that most impact on injectivity into the Wonnerup. Simulations combining the reservoir uncertainties were conducted to generate data for a probability distribution curve (Table 6). Figure 25 shows that at the P50 level of uncertainty, 6.1 million tonnes of gas (~560 tonnes/day/well) can be injected into the Wonnerup.

Scenario	Million Tonnes of CO2 Injected Over 30 Years
Low Krg	3.1
Small Compartment	3.6
Low BHP Constraint	4.3
Low Krw	4.6
Low Permeability	5.1
Low Vertical Permeability	6.6
Reference Case	6.9
Large Compartment	7.4
High Krw	7.8
High Permeability	9.0
High BHP Constraint	9.3
High Krg	9.8

**Table 5 Impact of Reservoir Uncertainties on Injectivity in the Wonnerup**

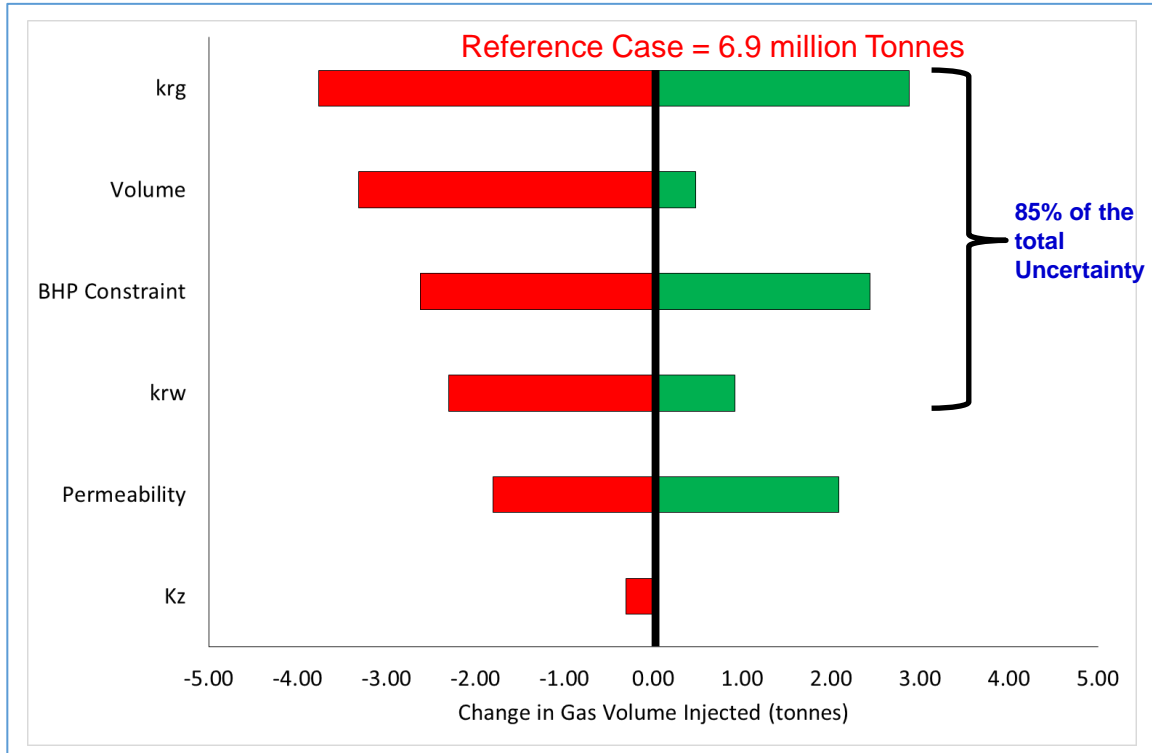
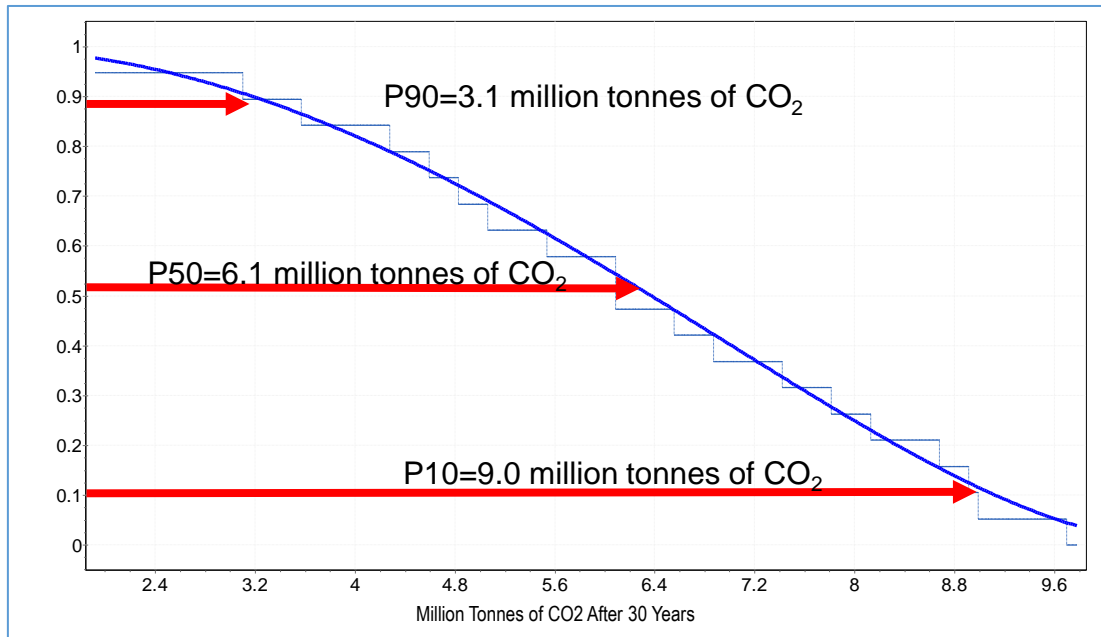


Figure 24 Tornado Chart Showing Impact of Reservoir Uncertainties on Injectivity



Scenario	Million Tonnes of CO2 Injected Over 30 Years
Low Krg Low BHP Constraint	1.92
Low Krg Low Krw	2.24
Small Compartment Low Krg	2.90
Low Krg	3.14
Small Compartment	3.59
Small Compartment Low BHP Constraint	3.59
Low BHP Constraint	4.28
Low Krg High Permeability	4.30
Low Krw	4.60
High Krw Low BHP Constraint	4.85
Low Permeability	5.10
High Permeability Low BHP Constraint	5.61
High Krg Low BHP Constraint	6.13
Low Vertical Permeability	6.60
Reference Case	6.90
Small Compartment High Permeability	7.12
Large Compartment	7.38
Low Permeability High Krg	7.44
High Krw	7.82
High Permeability	8.99
Low Vertical Permeability High Krg	9.28
High BHP Constraint	9.34
High Krg	9.78
High Krg High Permeability	12.34

**Table 6 Range of Gas injected – Combined Uncertainties**



**Figure 25 Probability Distribution of Injectivity Over 30 Years**

## 6. MODELLING OF THE CO<sub>2</sub> PLUME

---

This phase of the study is focussed on the full field modelling of the movement of the CO<sub>2</sub> plume after 30 years of injection at 800,000 tonnes per annum and 1000 years of shut-in. The full field model integrates all of the available subsurface information into a dynamic reservoir model that represents and describes the fluid flow processes in the reservoir.

To enable the simulations to be conducted in a reasonable time, a coarse scale model of the Harvey area was constructed to investigate plume movement in the Harvey area during and after injection of the planned CO<sub>2</sub> volume.

### 6.1 Simulator Selection

The full field model of the Harvey area was constructed in the compositional simulator, GEMS™ (Version 2015.10). GEMS<sup>ii</sup> is a full featured compositional simulator and capable of modelling:

- Hysteresis and residual gas trapping.
- Gas solubility in aqueous phase.
- Vaporization of water during CO<sub>2</sub> injection.
- Detailed calculations of brine density, viscosity and accounts for solubility of CO<sub>2</sub> in the brine.

### 6.2 Model Description

The model was constructed with grid blocks of 250X250 metres in the I- and J-directions with the resolution of the layers in the Yalgorup retained at the geological model scale of 1 metre. In the Wonnerup, the 4 metre layers were used (Figure 26). To further reduce the number of cells in the full field model, all cells with a depth shallower than 800 mTVDss was made void. Migration of CO<sub>2</sub> shallower than 800 mTVDss is considered a breach of containment as the CO<sub>2</sub> changes from a supercritical state to a gaseous state at depths shallower than 800 mTVDss.

---

<sup>ii</sup> GEMS is a trademark of Computer Modelling Group (CMG)

As most of the significant geological features in the Wonnerup and Yalgorup i.e. the width of the paleosols and channel belts are significantly wider than 250 metres the upscaling in the I- and J-directions from 25X25 metres to 250X250 metres is unlikely to affect the modelling of fluid flow in the I- and J- directions. Figure 27 shows that the permeability distribution in the I- and J- directions in the fine scale model (25X25 metres) and coarse scale model (250X250) are similar. Figure 28 shows the connected bodies from the fine and coarse scale models are similar.

The dimensions of the model are summarised below:

- 51 cells in the I-direction.
- 37 cells in the J-direction.
- 1050 cells in the K-direction.
- 1, 981, 350 cells of which 1, 024, 382 are active cells.
- Cell sizes of 250 m X 250 m X 1 m in the Yalgorup
- Cell sizes of 250 m X 250 m X 4 m in the Wonnerup
- The Yalgorup is modelled in Layers 1 to 700.
- The Wonnerup is modelled in Layers 701-1050.

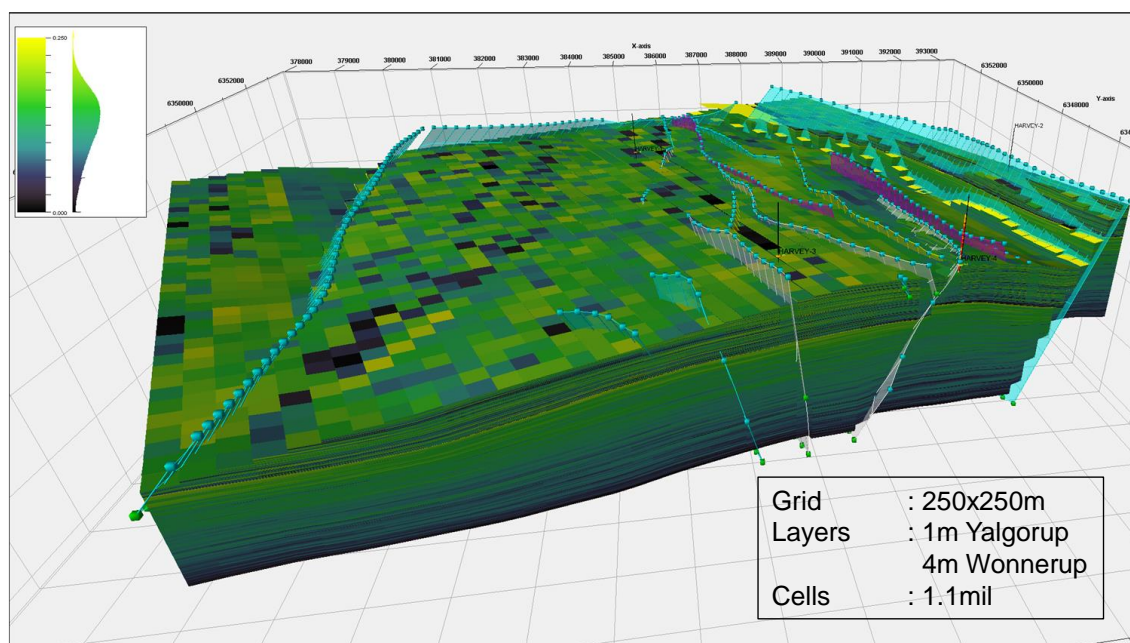
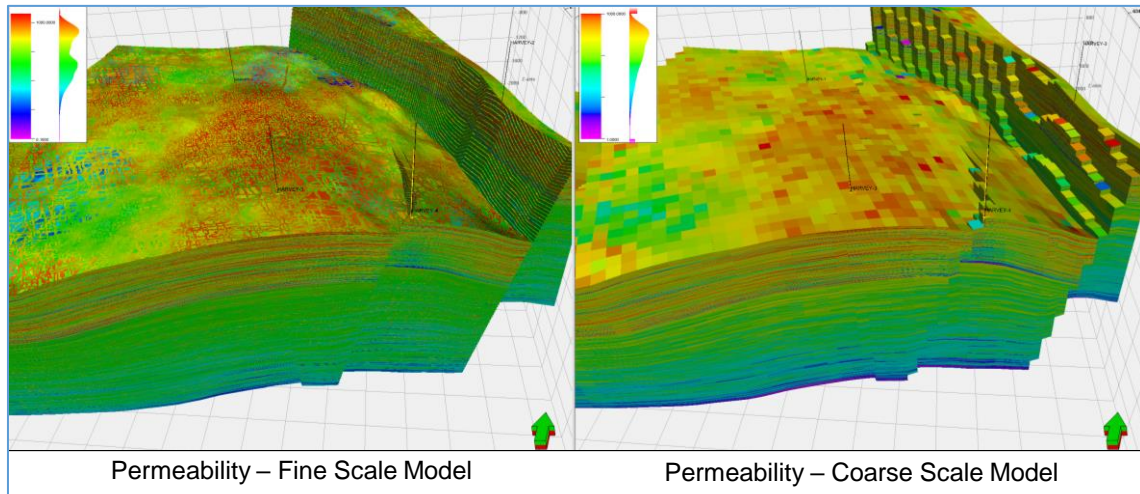
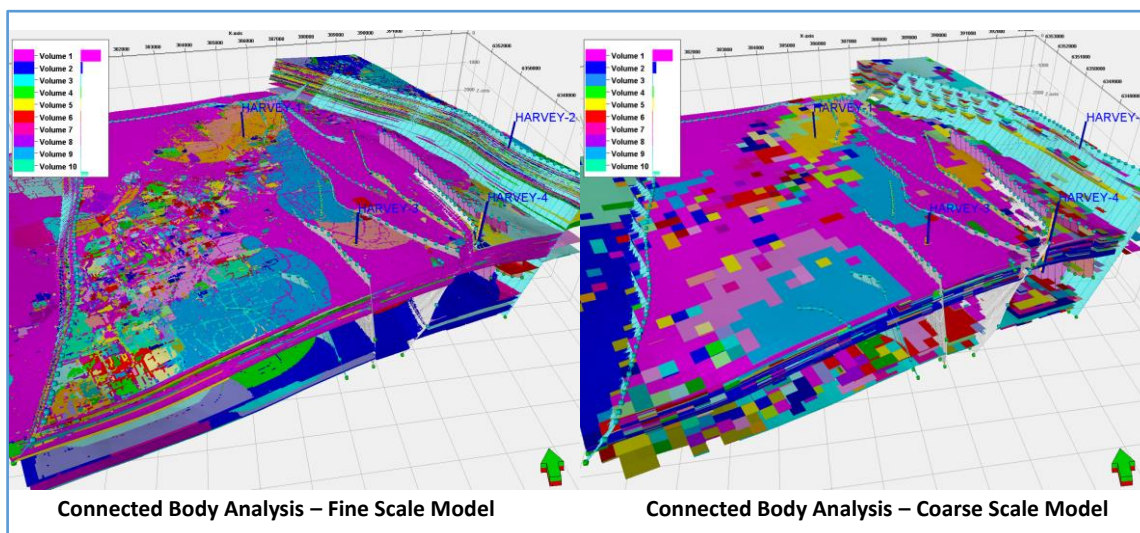


Figure 26 Coarse Scale Model Showing Porosity Distribution



**Figure 27 Comparison of Permeability Distribution - Fine and Coarse Scale Models**



**Figure 28 Connected Body Analysis - Fine and Coarse Scale Models**

### 6.3 Initialisation Parameters

The full field model was initialised with the following parameters:

- Initial Pressure
  - Initial pressure based on the RCI data from Harvey-1.
  - Reference pressure of 19327 kpa at 1900 metres.
- Reservoir Temperature
  - Temperature varies with depth.
  - At 800 metres the temperature is 44 °C.
  - At 3000 metres the temperature is 76 °C.

- The model was initialised as completely water saturated.

## 6.4 PVT Model

The PVT model used in the simulation is a CO<sub>2</sub>- Brine model with a salinity of 46<sup>iii</sup> g/l H<sub>2</sub>O NaCl Equivalent. Solubility of CO<sub>2</sub> in the brine is calculated using Henry's Law.

## 6.5 Aquifer Extent

The full field model of the Harvey area by no means captures the full extent of the Wonnerup and Yalgorup aquifers. Figure 29 shows that the Yalgorup and Wonnerup (Reference 7) are unconstrained at least 50 km to the north and 25 km to the south of the area of interest. To model the likely extent of the aquifer the pore volume of the columns at the end of the model were increased (Figure 30) using multipliers.

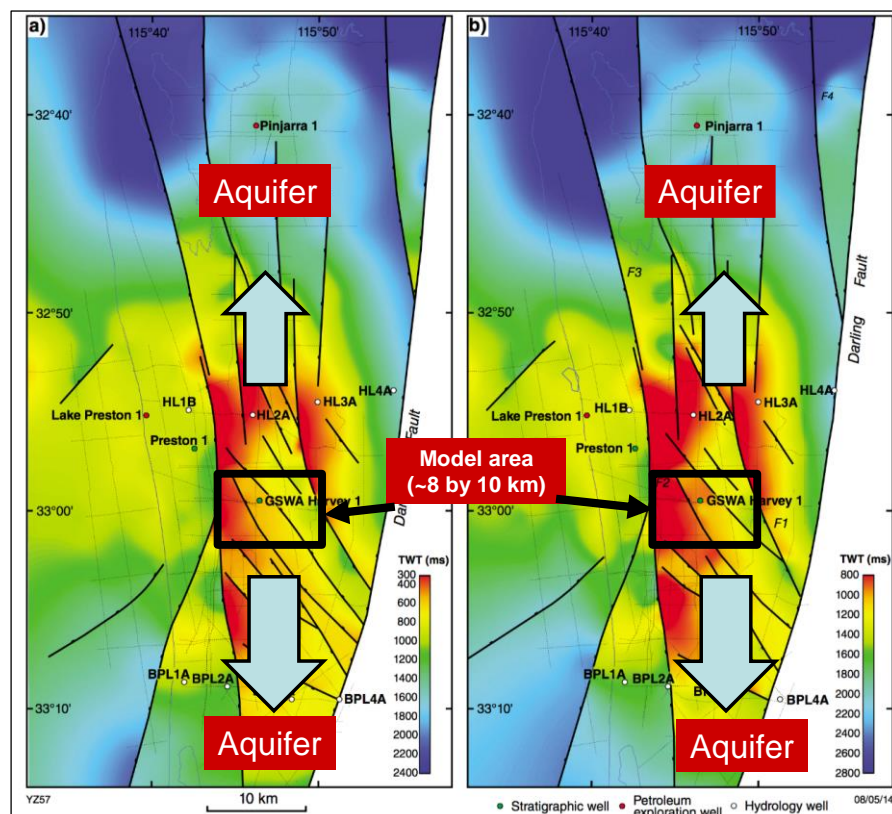


**Figure 29** Time Structure maps of the: a) top Yalgorup Member; b) top Wonnerup Member (After Reference 7)

<sup>iii</sup> The simulation model used the synthetic sample from Core Laboratories.

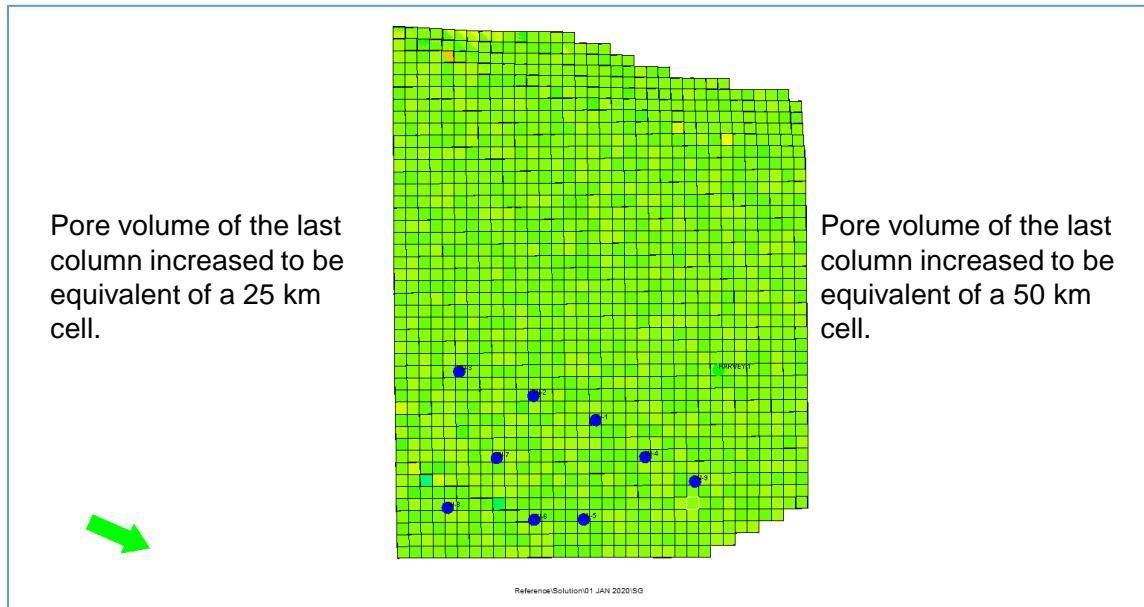


**Figure 30 Modelling the Extent of the Wonnerup and Yalgorup Aquifers**

## 6.6 Reservoir Properties

Reservoir properties such as permeability, porosity, net sand and structural information were imported directly from Petrel. Figure 31 to Figure 33 show the permeability and porosity distribution in the Harvey model. It should be noted that there are no obvious vertical or horizontal permeability barriers. Figure 33 shows that the porosity of the Wonnerup deteriorates towards the base and results in lower permeability in the base of the reservoir. The anomalously high porosities observed at the base of the Wonnerup in Harvey-1 have been excluded from the porosity distribution in the model (Reference 8).

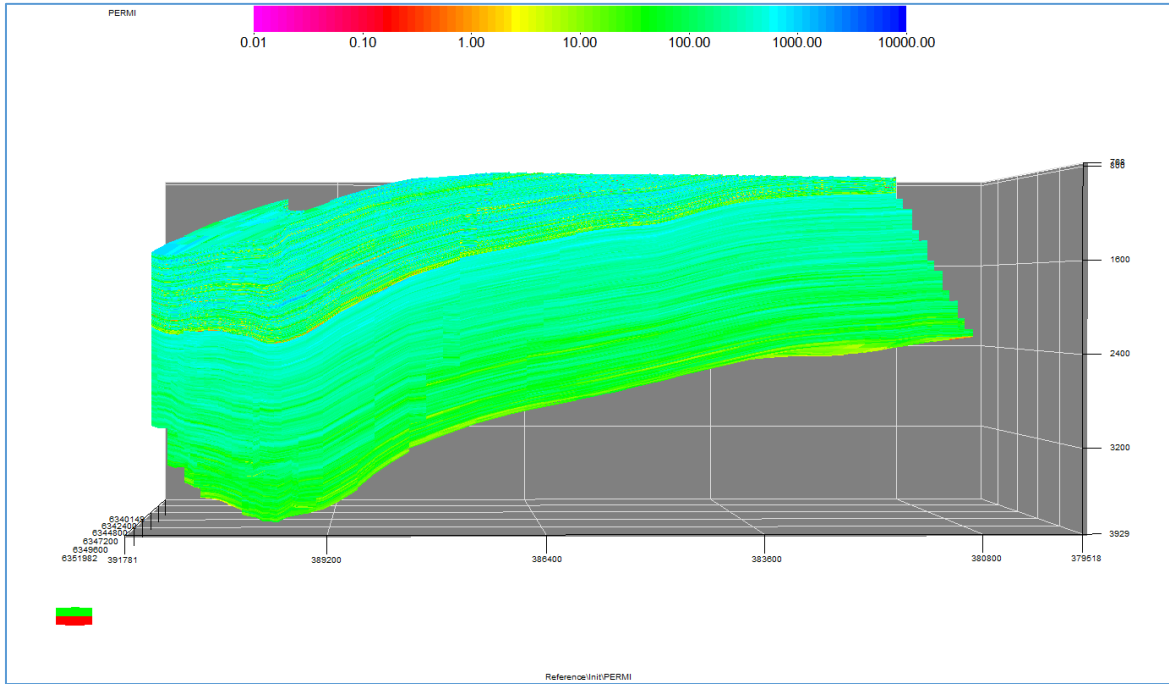


Figure 31 X-Section through the Harvey Full Field Model – Horizontal Permeability

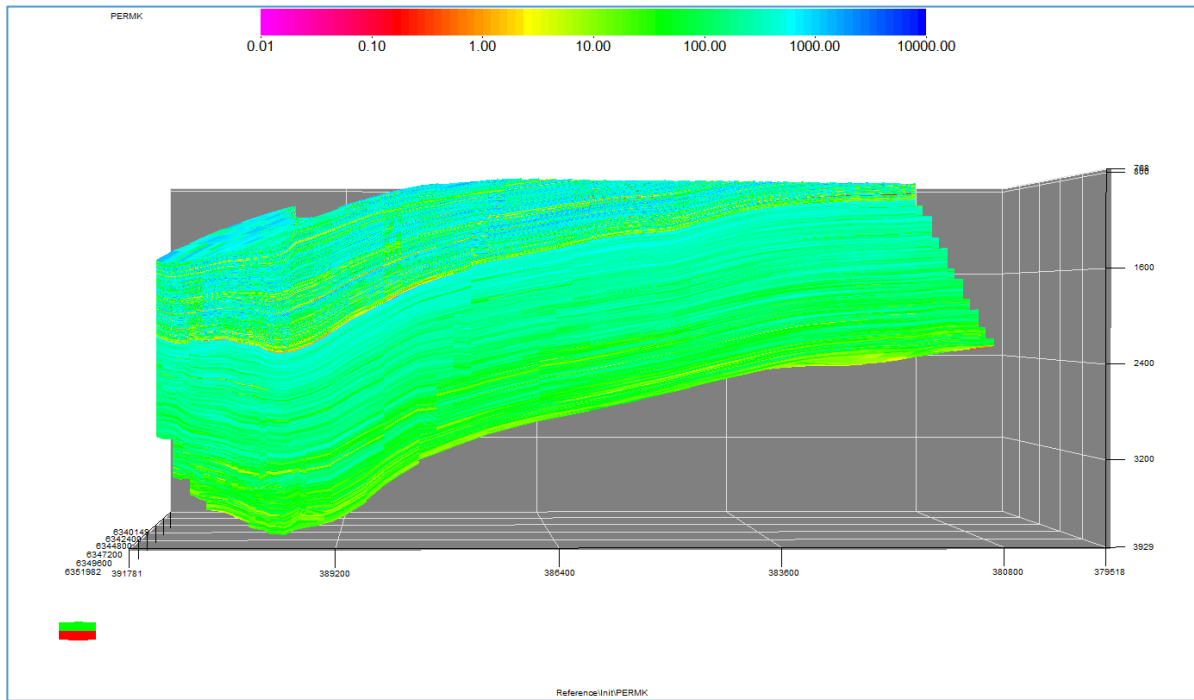
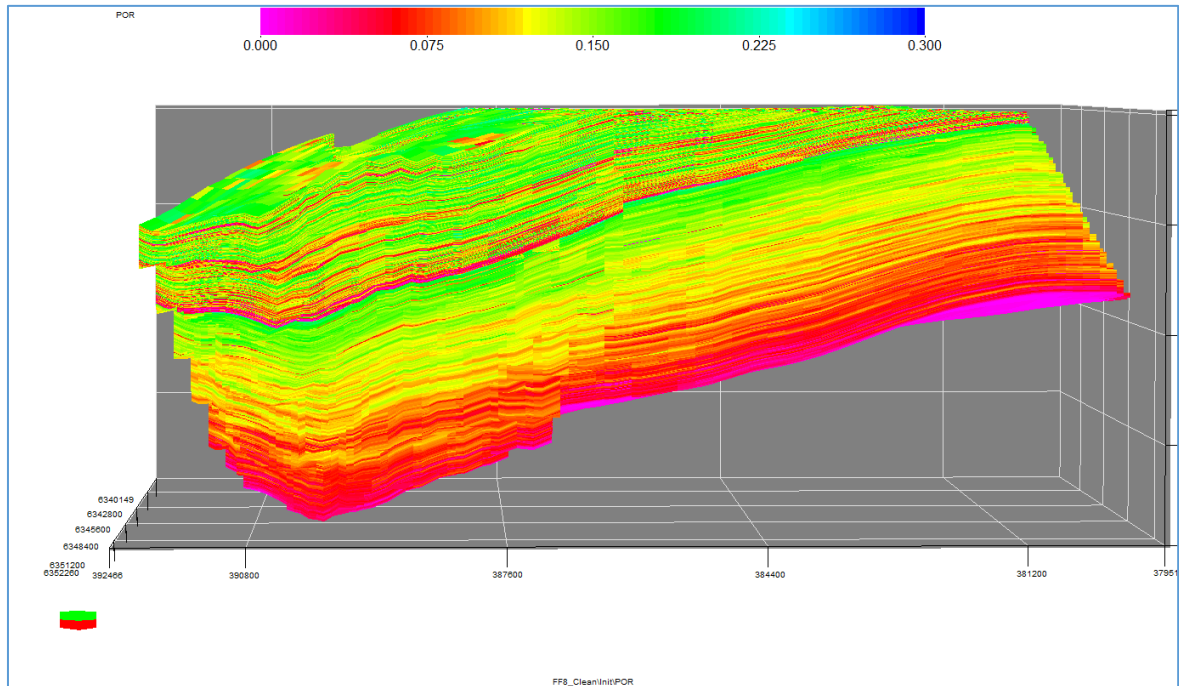


Figure 32 X-Section through the Harvey Full Field Model – Vertical Permeability



**Figure 33 X-Section through the Harvey Full Field Model – Porosity**

## 6.7 Conceptual Development Plan – Reference Case

The conceptual development plan for the Harvey area envisages injection of 800,000 tonnes of CO<sub>2</sub> per year for 30 years. At the end of the 30 year injection period, the wells are shut-in and the CO<sub>2</sub> is allowed to dissipate through the aquifer. In this work, it was assumed that 9 wells laid out in a staggered line-drive configuration would be used to inject CO<sub>2</sub> into the Wonnerup reservoir. All of the wells are completed in the bottom 250 metres of the Wonnerup.

### 6.7.1 Reference Case Definition

The Reference Case for the conceptual development study is defined as follows:

- Reservoir
  - All faults are assumed to be not sealing.
  - Wonnerup and Yalgorup are assumed to be in communication.
- PVT Properties
- NaCl concentration of 46 g/L H<sub>2</sub>O.



- No mineralisation is assumed.
- Model includes the solubility of CO<sub>2</sub> in brine.
- Injection fluid assumed to be 100% CO<sub>2</sub>.
  
- Rock-Fluid
  - Hysteresis of the gas phase is assumed.
  - Trapped gas saturation,  $S_{gT} = 0.19$
  - No hysteresis of the water phase
  
- Injection
  - CO<sub>2</sub> is injected at rate of 800,000 tonnes per annum through 9 wells.
  - Injection begins on an arbitrary date of 1/1/2020 and ends on 10/1/2050.
  - Bottom hole pressure constraint = 360 bars @ 2948 m [Pore Pressure + 0.9\*69 bars]
  
- In the simulation model, relative permeability curves were generated using the following Corey exponents and end points:
  - $N_w = 4.0$
  - $N_g = 4.5$
  - $K_{rw} @ (S_w=1) = 0.37$
  - $K_{rg} @ (S_{wmin}=0.49) = 0.12$

## 6.7.2 Results

Figure 34 shows the injection performance of the Reference Case. The results of the modelling show that 800,000 tonnes/year of CO<sub>2</sub> was injected into the Wonnerup in the model for 30 years for a cumulative injection of 24 million tonnes of CO<sub>2</sub>. The bottom hole pressures during the injection period (Figure 35) are never close to the bottom hole pressure constraint.

Figure 36 and Figure 37 show the CO<sub>2</sub> distribution in the water phase at two instances of time: after 30 years of injection and after 1000 years after injection. The plots show that the CO<sub>2</sub> front does not reach the location of Harvey-1 even after 1000 years. Figure 38 is an E-W cross section through two HI-2 and HI-6 showing that the CO<sub>2</sub> front rose to a depth ~620 metres below the top of the Wonnerup and that the injected CO<sub>2</sub> volume does not migrate beyond the Wonnerup. The results of the modelling also show that the

movement of CO<sub>2</sub> in the model effectively stops after about 500 years and suggests that modelling could be terminated after 500 years of simulation time.

The material balance accounting of the CO<sub>2</sub> injected in the Reference Case model after 1000 years (Table 7) show that about 56% of injected CO<sub>2</sub> is dissolved in water. The remainder is in a supercritical phase.

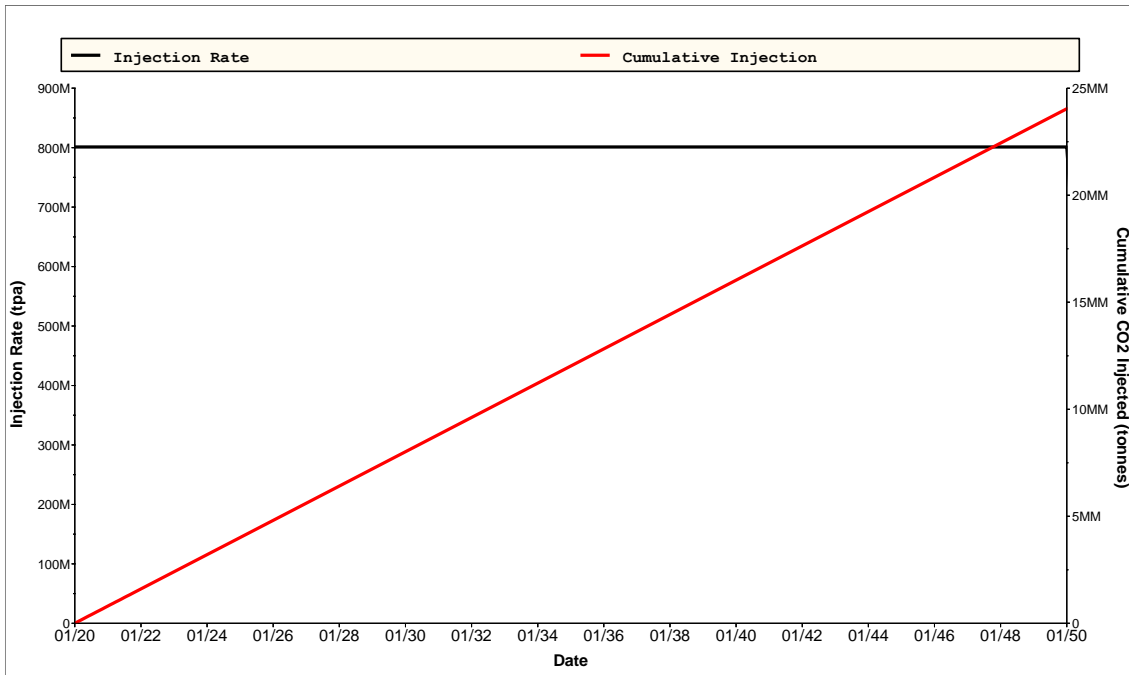


Figure 34 Injection Performance – Reference Case

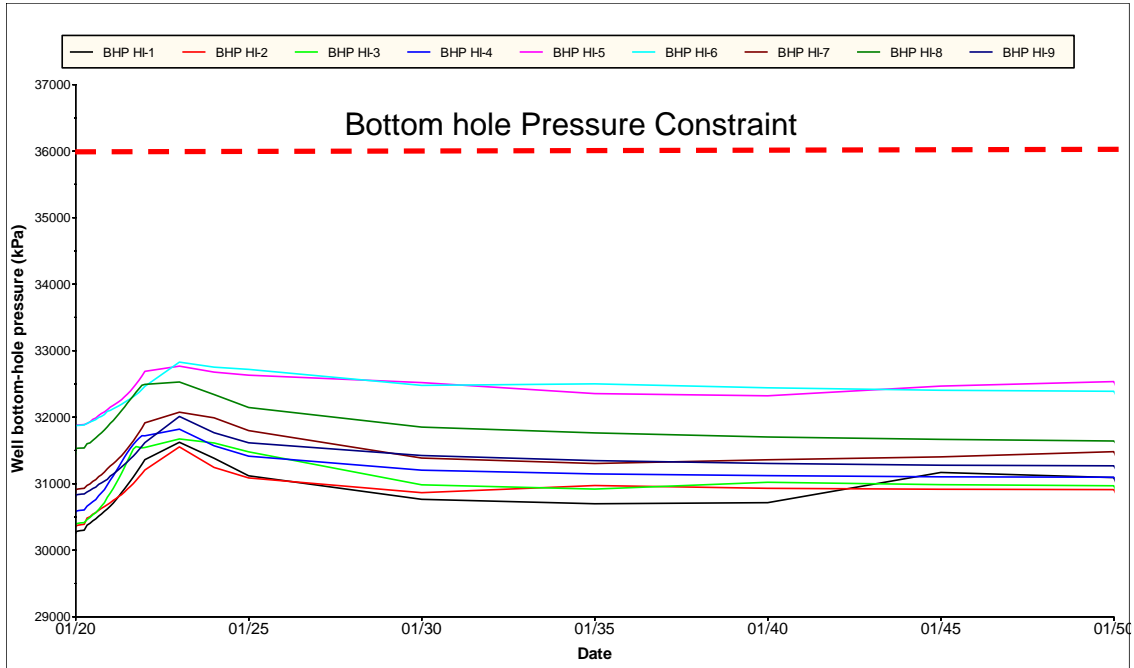


Figure 35 Bottom Hole Pressure Profile by Well During Injection – Reference Case

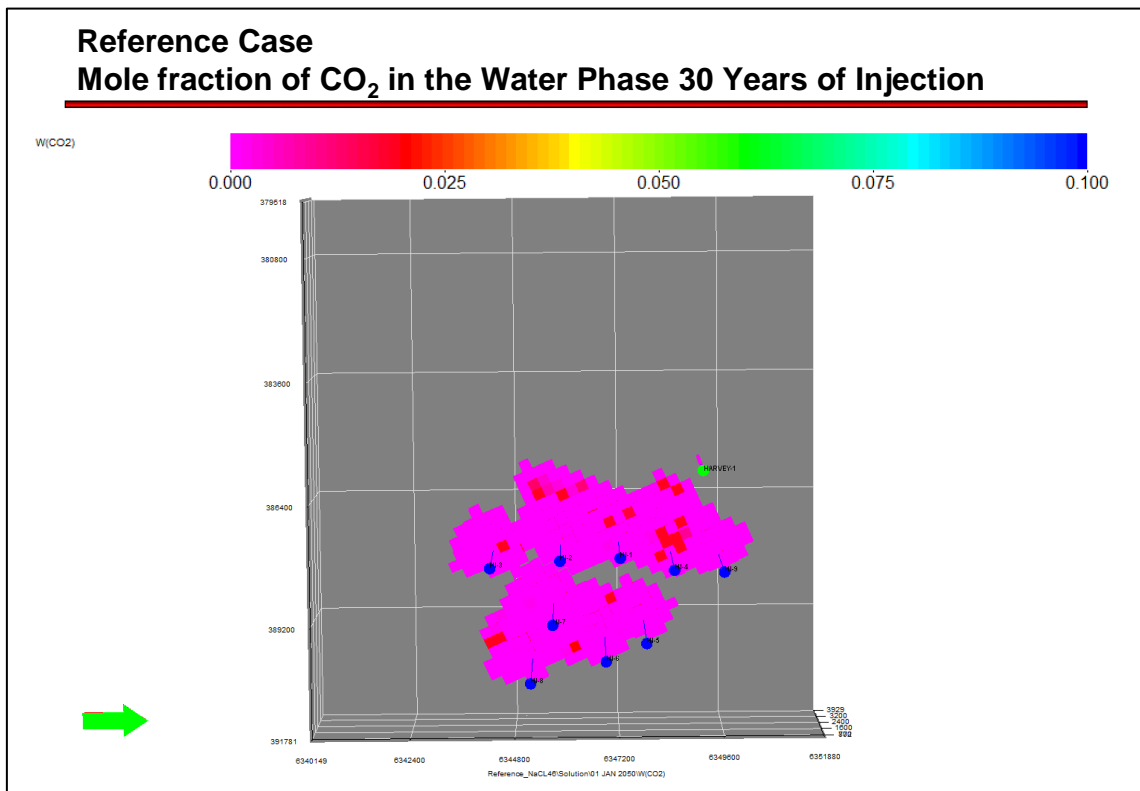


Figure 36 Top View – Reference Case CO<sub>2</sub> Distribution at end of Injection Period

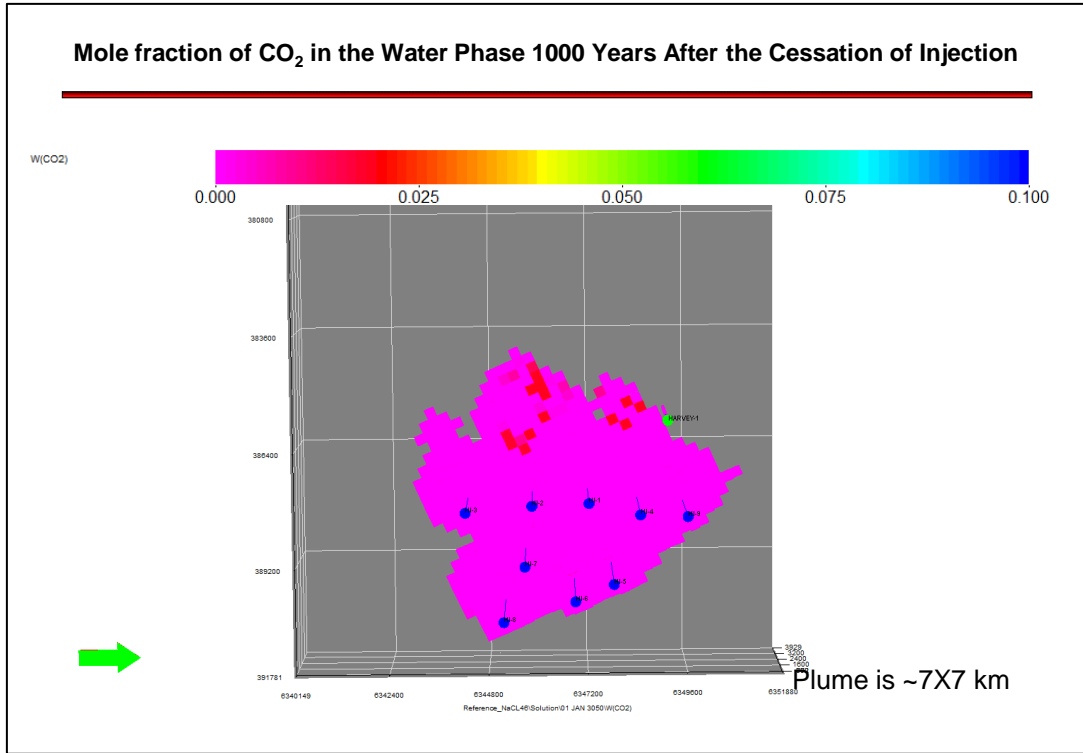


Figure 37 Top View – Reference Case CO<sub>2</sub> Distribution 1000 years after injection

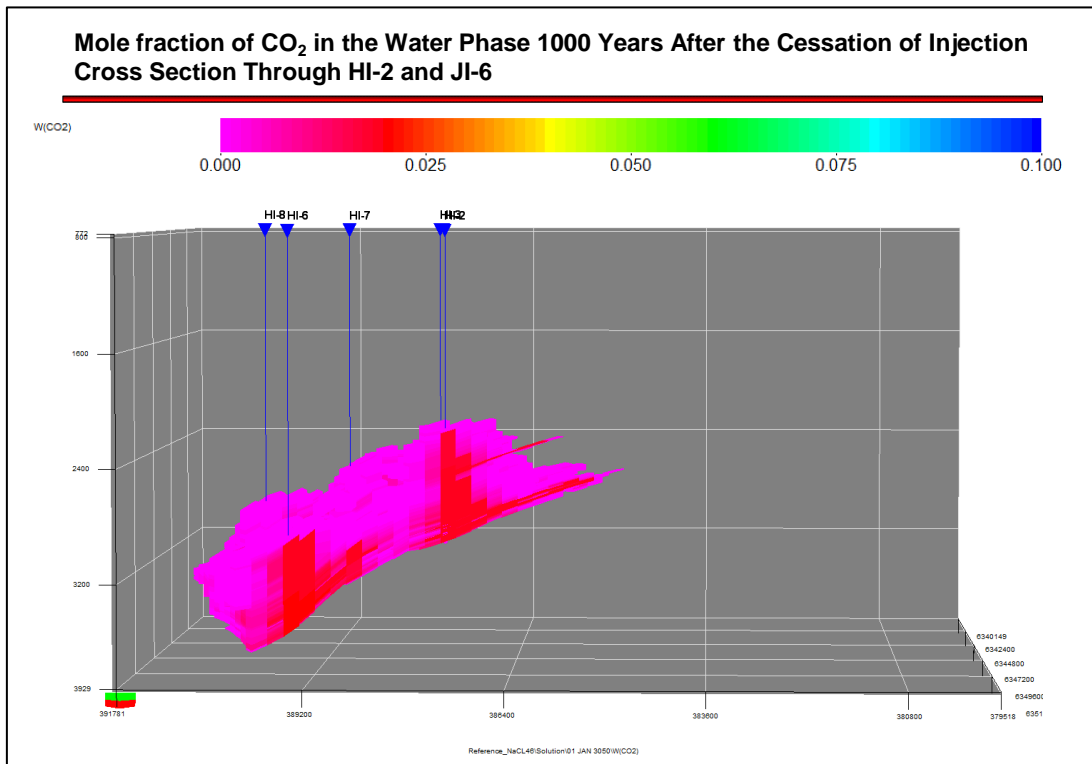


Figure 38 Reference Case – X-Section through HI-2 and HI-6

CO <sub>2</sub> Storage Amounts in the Reservoir	Moles	% of Moles Injected
Gaseous Phase	0	0%
Liquid Phase	0	0%
Dissolved in Water	3.13E+11	55%
Total Supercritical Phase	2.58E+11	45%
Supercritical Phase Trapped (Sgc or Hysteresis)	2.52E+11	44%
Supercritical Phase not trapped	6.00E+09	1%

Table 7 Material Balance Accounting (1000 Years after Injection)

## 6.8 Impact of Reservoir Uncertainties on the movement of the CO<sub>2</sub> plume

A number of models of the Harvey area were constructed to investigate the effects of the reservoir uncertainties on containment failure and the location of the CO<sub>2</sub> plume in relation to the abandoned Harvey-1 well. Table 8 is a summary of the reservoir uncertainties investigated and the parameters used in the investigations.

Case	Model Name	Geological Model	Trapped Gas Saturation	Brine Salinity (g/L NaCl Eq.)	Internal Faults	End Point Gas Relative Permeability
Reference	Reference	Reference	0.19	45600	Not sealing	0.12
1	Holey Faults	Vertical permeability of cells adjacent to faults is increased by 10 times.	0.19	45600	Not sealing	0.12
2	HighKrg	Reference	0.19	45600	Not sealing	0.23
3	LoHyst	Reference	0.10	45600	Not sealing	0.12
4	HighPerm	Proportion of High Energy Facies in Wonnerup increased to 90%.	0.19	45600	Not sealing	0.12
5	Hikvkh	Vertical and horizontal permeability are equal.	0.19	45600	Not sealing	0.12
6	Seismic_Trend	Used Seismic Trend (Deterministic Case) to populate Paleosols in the Wonnerup.	0.19	45600	Not sealing	0.12
7	Fault_Trans	Reference	0.19	45600	Fault transmissibility multiplier of 0.1	0.12
8	LoSol	Reference	0.19	200000	Not sealing	0.12

Table 8 Case Summary – Full Field Model of the Harvey Area

### 6.8.1 Case 1 – High Vertical Permeability (“Holey Faults”)

The area of interest in the Harvey area is intersected by a number of faults. None of these faults are expected to form lateral barriers to flow but the areas near the faults may have enhanced vertical permeability due to fractures. In Case 1, these fracture zones are modelled as areas of enhanced vertical permeability. The vertical permeability of cells adjacent to a fault are increased 10 times.

Figure 40 compares the distribution of CO<sub>2</sub> in the Reference Case and Case 1 after 500 years. The distribution of CO<sub>2</sub> in Case 1 is more compact compared to the Reference Case as a result of the CO<sub>2</sub> being more evenly distributed in the shallower layers (Figure

41) as evidenced by the lack of pronounced humps in the CO<sub>2</sub> profile. The high permeability conduits included in the model have little impact on the vertical migration CO<sub>2</sub>.

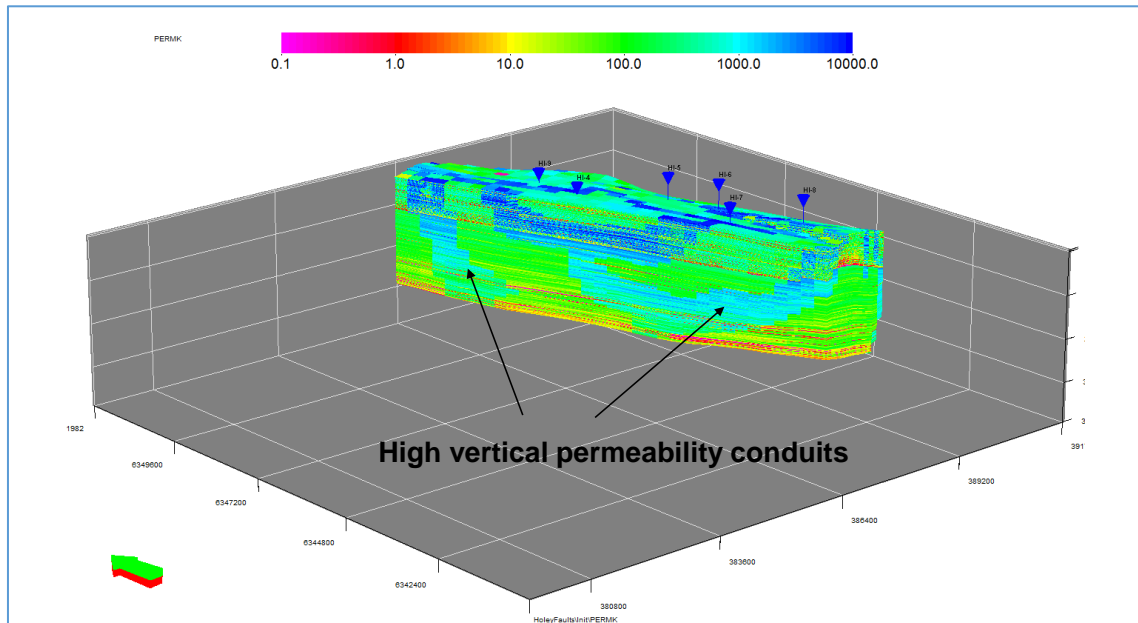


Figure 39 X-Section (I=35) through the model showing high permeability conduits

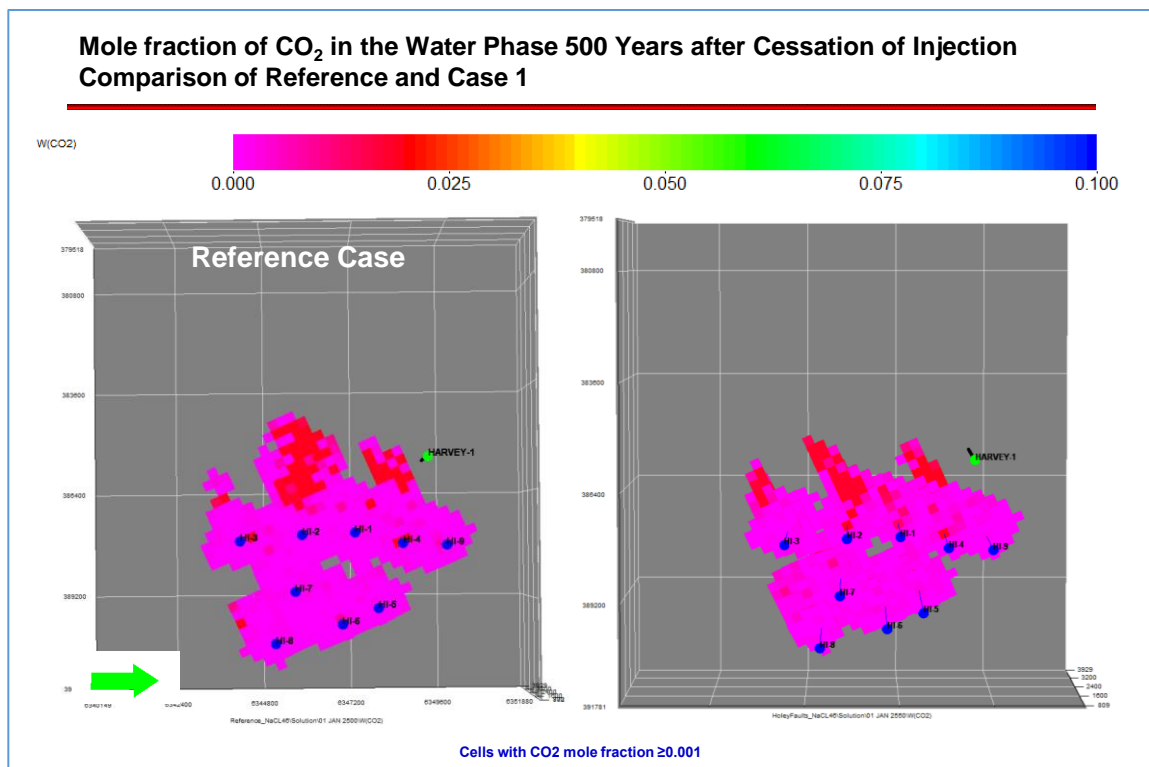
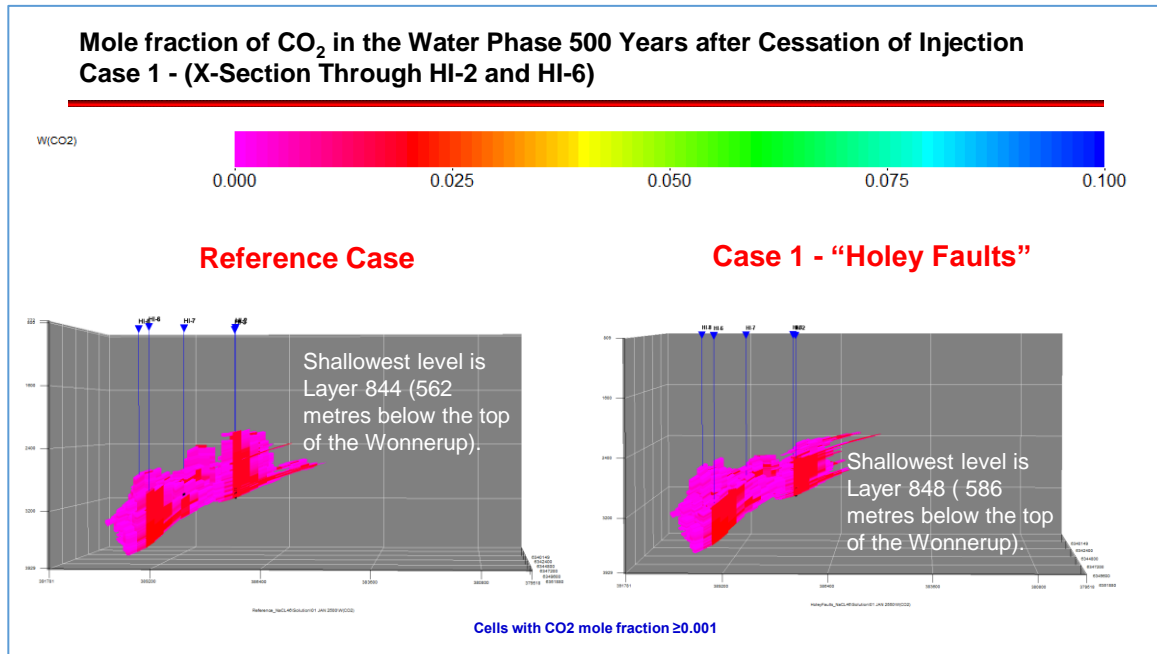


Figure 40 Top View – CO<sub>2</sub> Distribution (Comparison of Reference Case and Case 1)



**Figure 41 X-Section View – CO<sub>2</sub> Distribution (Comparison of Reference Case and Case 1)**

### 6.8.2 Case 2 – High Gas Relative Permeability ( $k_{rg}=0.23$ )

In this case, the end point relative permeability to gas,  $k_{rg}$ , was increased from 0.12 to 0.23 (Figure 42). Figure 43 shows that the increase in end point gas relative permeability has resulted in the CO<sub>2</sub> plume spreading farther towards the southwest and north but otherwise the aerial dimensions of the plume is not very different from the Reference Case. Figure 44 shows that the plume has migrated to shallower depths but is still deeper than 2000 mTVDss.

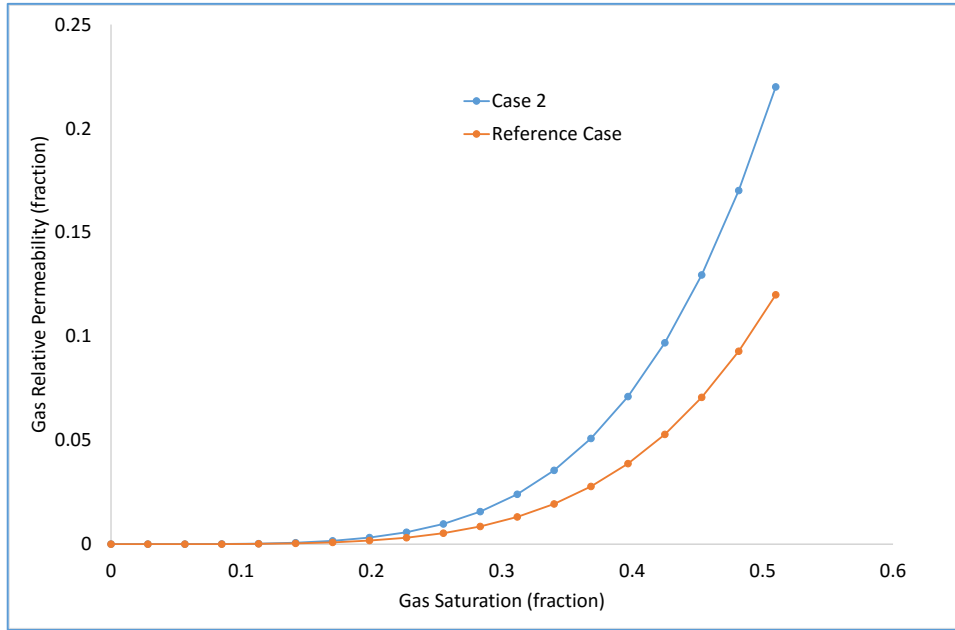


Figure 42 Gas Relative Permeability (Comparison of Reference Case and Case 2)

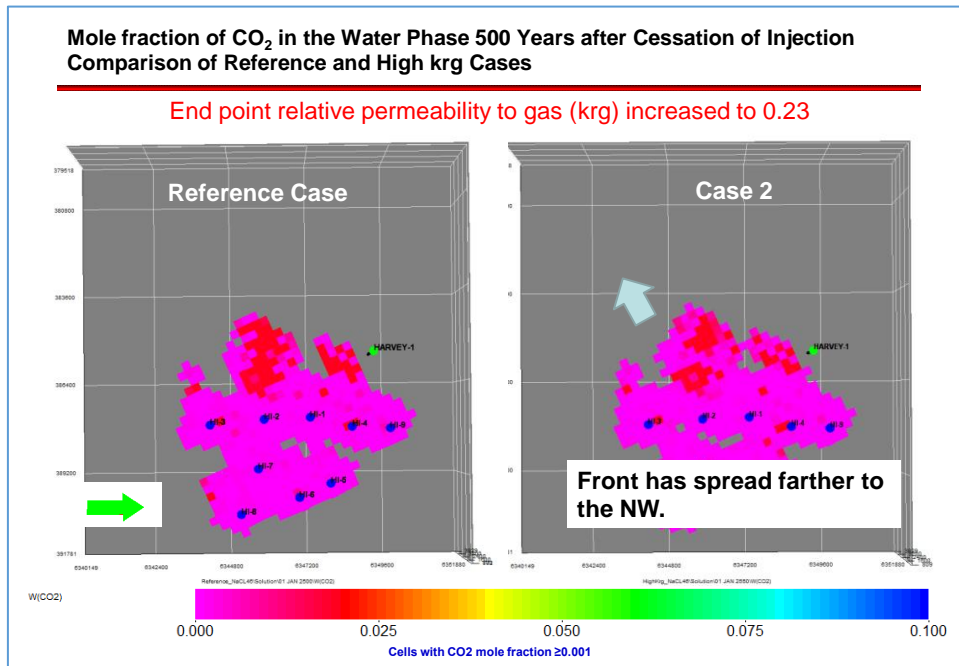


Figure 43 Top View – CO<sub>2</sub> Distribution (Comparison of Reference Case and Case 2)



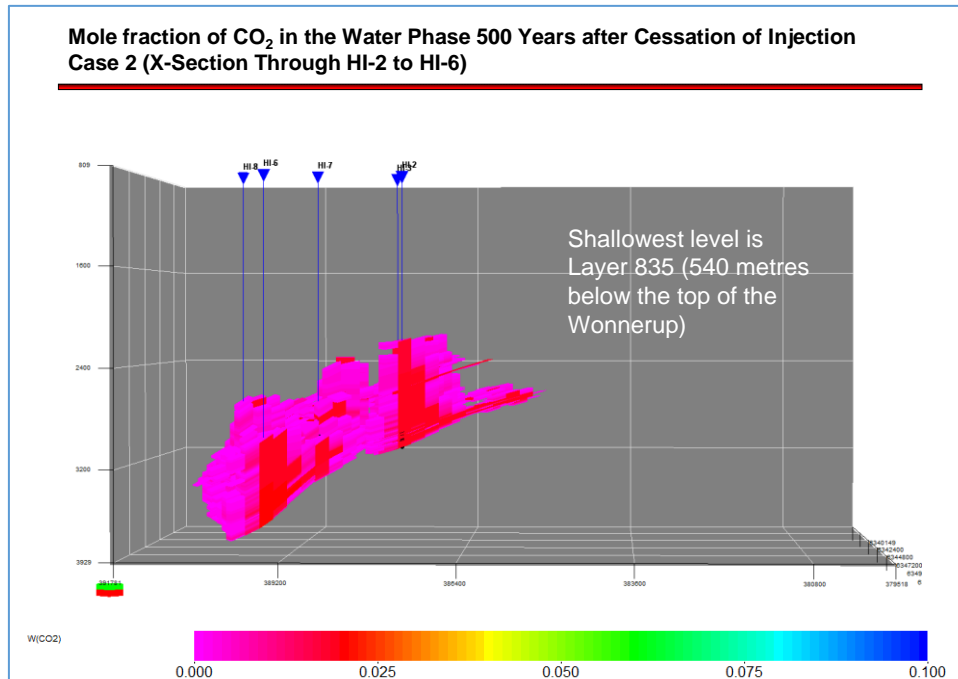


Figure 44 X-Section View – CO<sub>2</sub> Distribution (Case 2)

### 6.8.3 Case 3 – Low Trapped Gas Saturation ( $S_{gT}=0.10$ )

Steady state imbibition tests show the maximum trapped gas saturation to be about 0.19. Trapped gas saturation values of 25-30% are often measured on comparable sands in gas reservoirs. Although it is unlikely that trapped gas saturation would be much lower than 0.19, the impact on plume movement of lower trapped gas saturation was investigated. In Case 3, a trapped gas saturation value of 0.10 was investigated.

Figure 45 compares the spread of CO<sub>2</sub> in the Reference Case and Case 3. The lower trapped gas saturation has little impact on the lateral movement of the CO<sub>2</sub> front. Figure 46 shows that the lower trapped gas saturation has resulted in more vertical migration of CO<sub>2</sub> and that the plume is about 30 metres shallower (530 metres below the top Wonnerup) compared to the Reference Case.

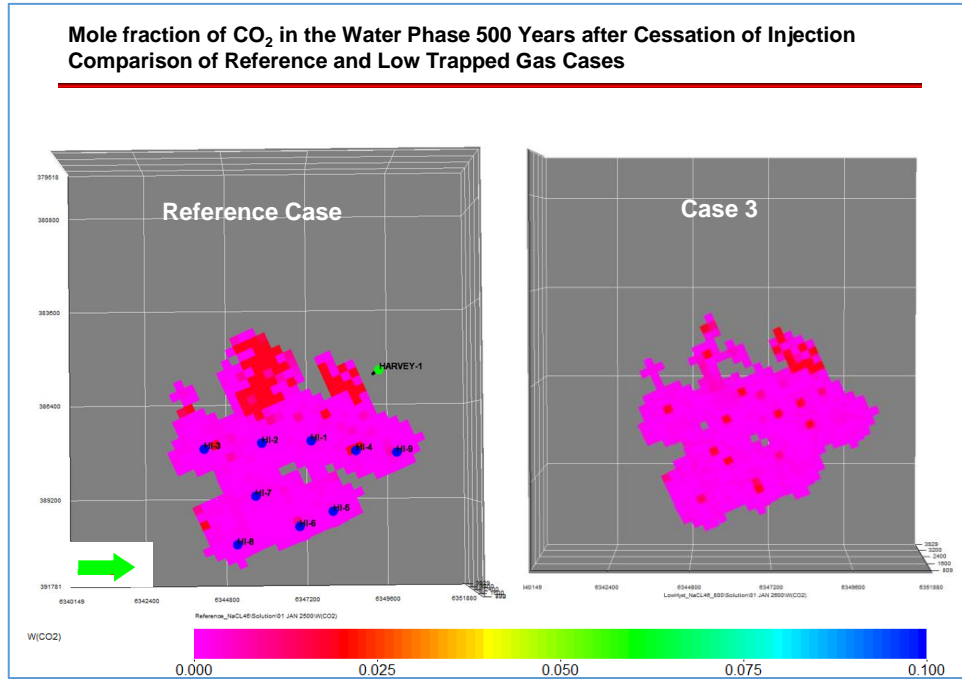


Figure 45 Top View – CO<sub>2</sub> Distribution (Comparison of Reference Case and Case 3)

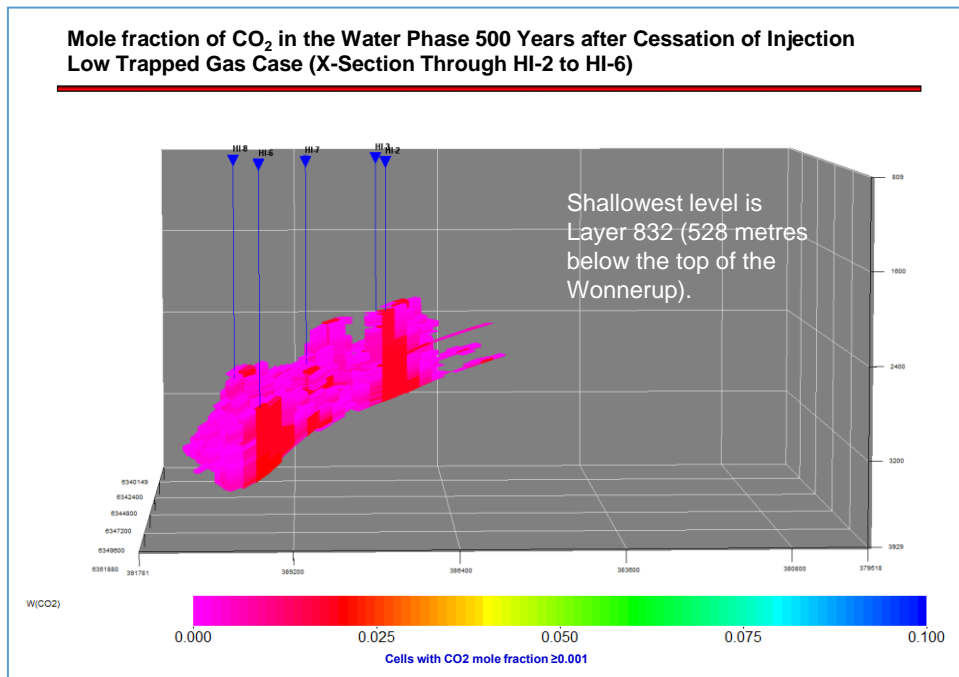


Figure 46 X-Section View – CO<sub>2</sub> Distribution (Case 3)

### 6.8.4 Case 4 - High Permeability Case

In this scenario, the proportion of high energy facies in the Wonnerup was increased to 90%. This has resulted in an increase in the average permeability to 357 mD compared to 199 mD in the Reference Case. Figure 47 shows that the CO<sub>2</sub> plume has not spread

as much to the SW but towards the North and Northwest. This spread towards the North and Northwest means that the plume has not migrated as much vertically.

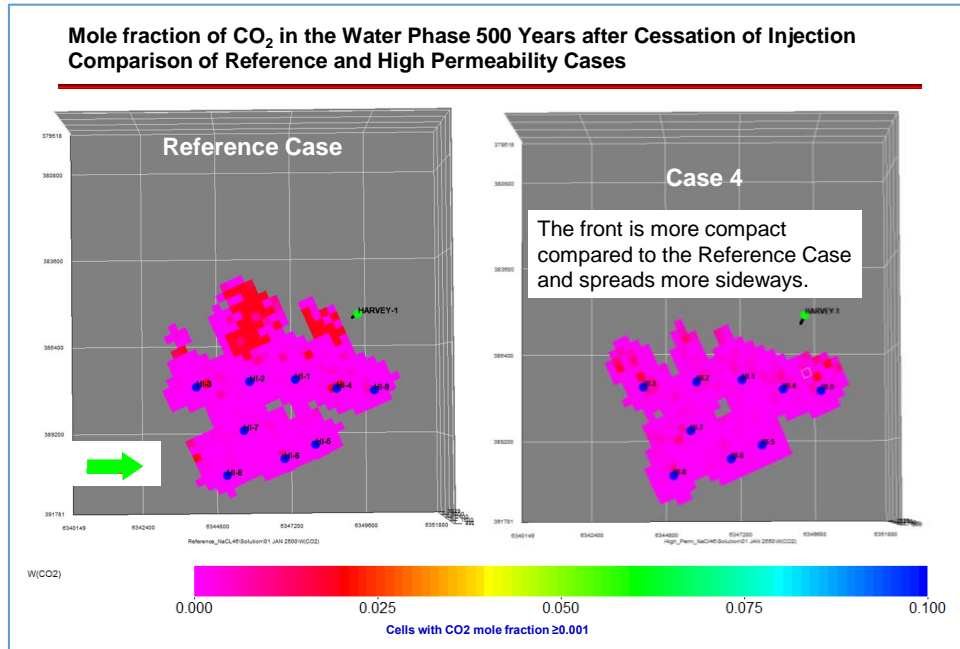


Figure 47 Top View – CO<sub>2</sub> Distribution (Comparison of Reference Case and Case 4)

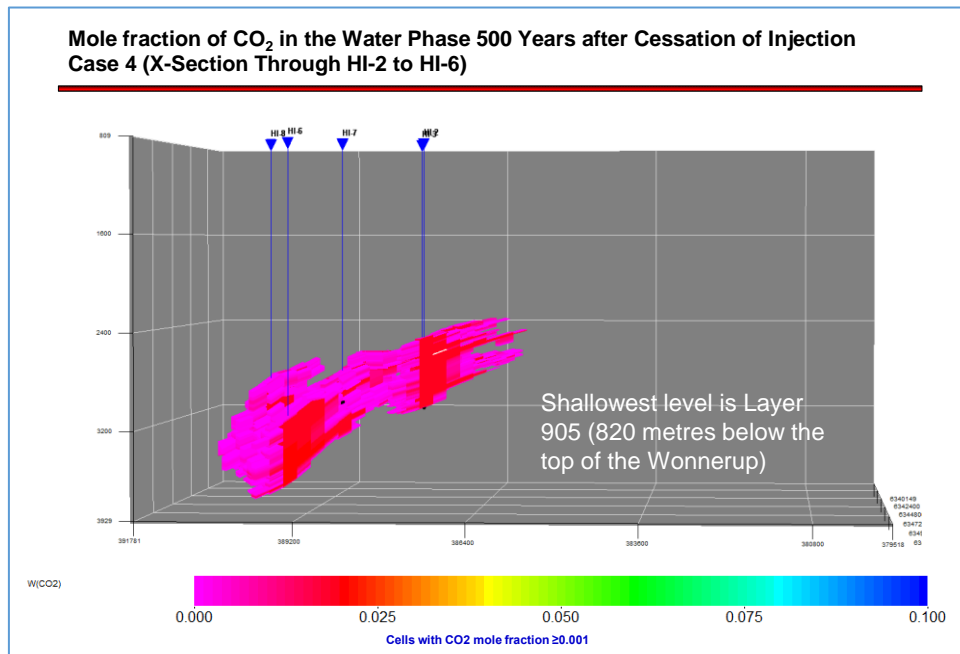


Figure 48 X-Section View – CO<sub>2</sub> Distribution (Case 4)

### 6.8.5 Case 5 – High kv/kh (Vertical to Horizontal Permeability Ratio)

In this scenario the vertical permeability in the cells are made equal to the horizontal permeability in the fine scale Petrel model and the upscaled permeability is imported into the simulation model. This increased the kv/kh from 0.91 in the Reference Case to 1.0 in Case 5. Figure 49 shows that the increase in kv/kh has little impact on the aerial extent of the CO<sub>2</sub> plume. The increase in kv/kh did promote the migration of CO<sub>2</sub> vertically (Figure 50) but the effect was modest.

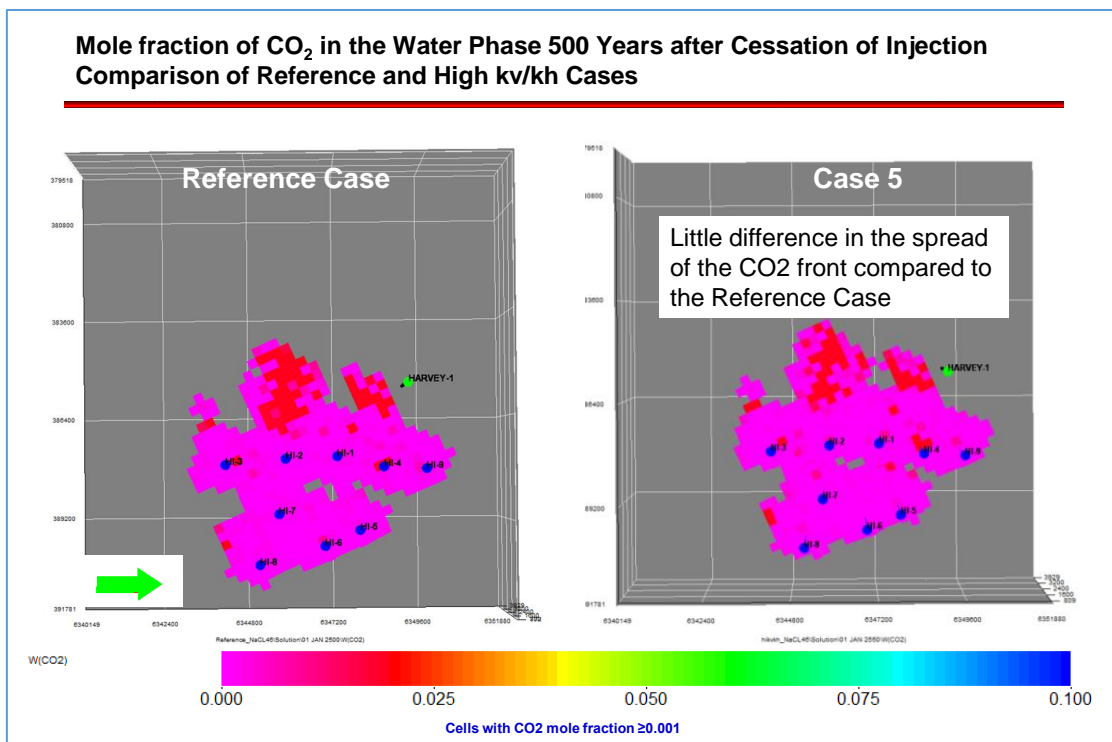
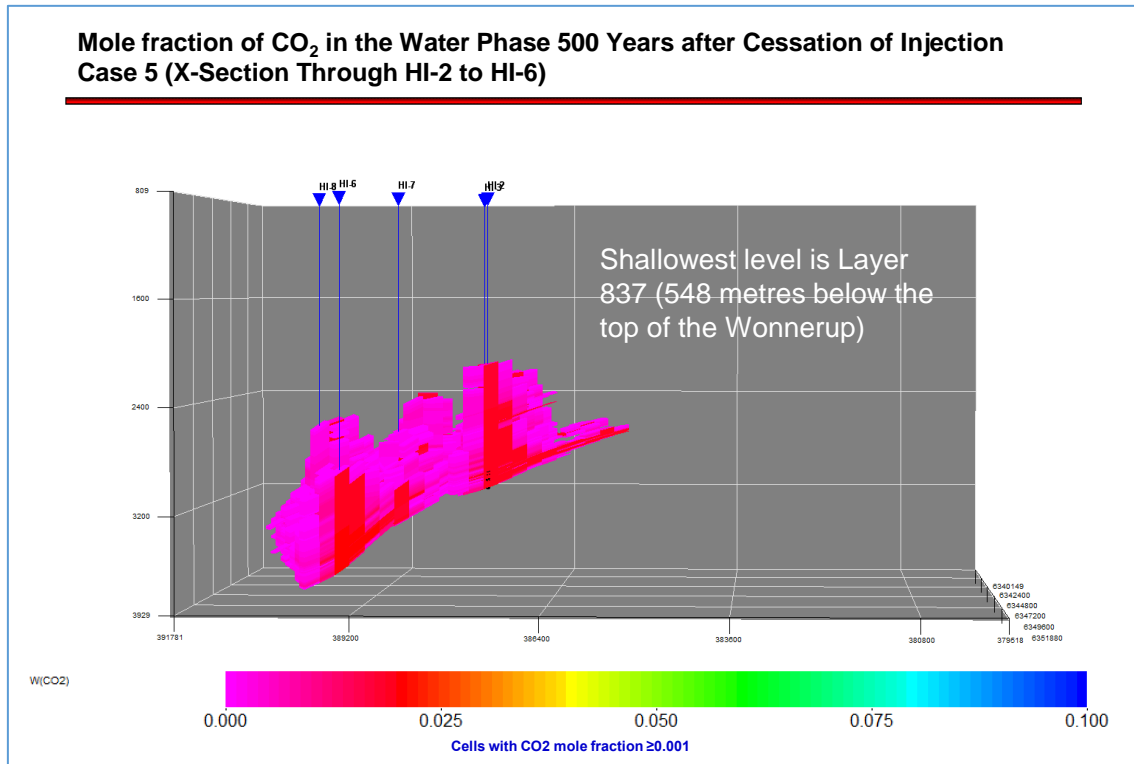


Figure 49 Top View – CO<sub>2</sub> Distribution (Comparison of Reference Case and Case 5)



**Figure 50 X-Section View – CO<sub>2</sub> Distribution (Case 5)**

### 6.8.6 Case 6 – Deterministic Scenario

In this scenario, the seismic trend is used to populate the paleosols in the Petrel model. Harvey-1 is the only well that has penetrated the full thickness of the Wonnerup sands. The data from the well shows the Wonnerup to have a high proportion of sand and relative homogeneous (Figure 51). This is consistent with the seismic data which is relatively bland in the area in which Harvey-1 is located. Towards Harvey-4, the seismic data becomes noisier and suggests a possible change in the character of the reservoir. To model this change in character the Wonnerup in the Petrel model was deterministically populated with paleosols.

Figure 52 shows that the shape of the CO<sub>2</sub> plume has changed significantly and is more compact because of the distribution of the paleosols. The compactness of the CO<sub>2</sub> plume means that more of the CO<sub>2</sub> migrates vertically (Figure 53).

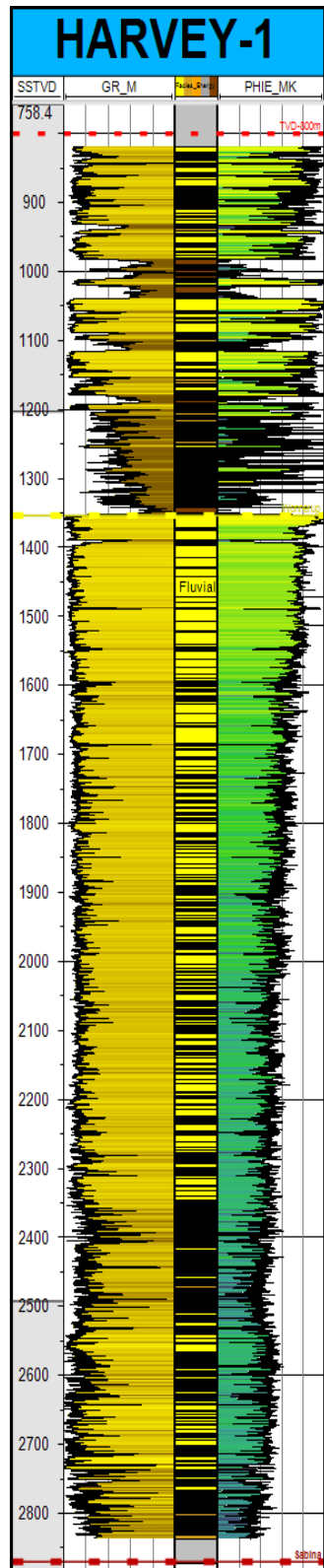


Figure 51 Harvey-1 – Gamma ray and interpreted porosity log.

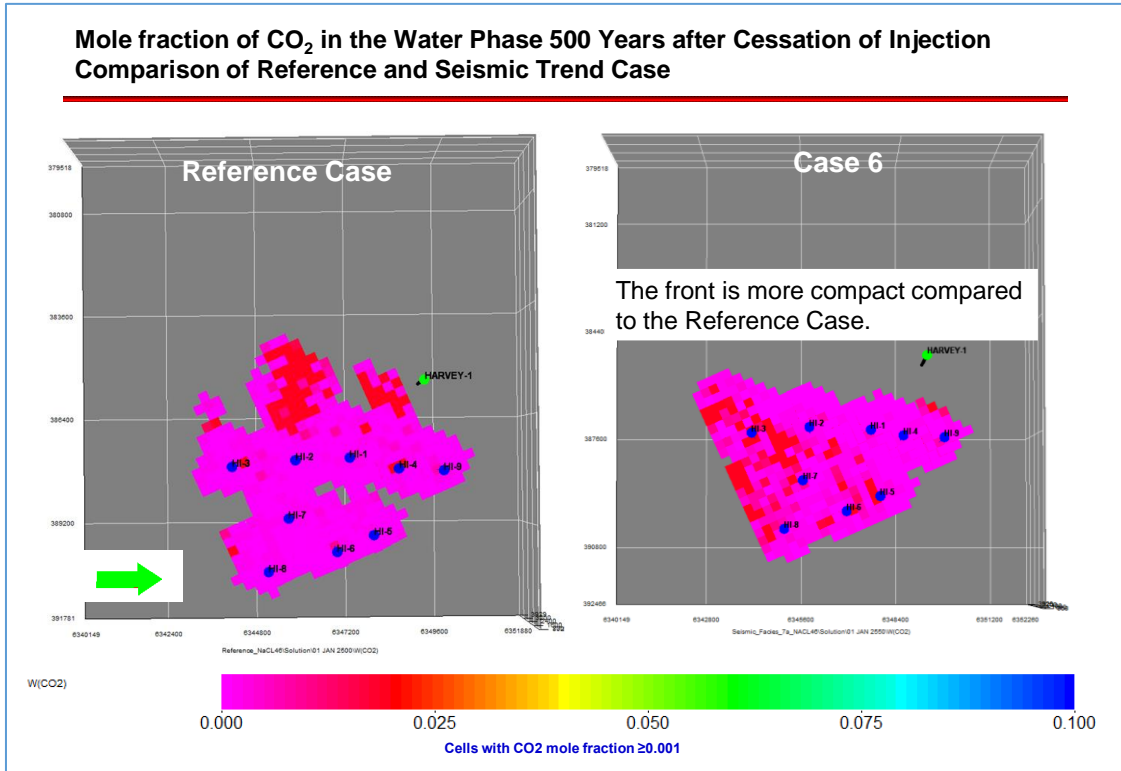


Figure 52 Top View – CO<sub>2</sub> Distribution (Comparison of Reference Case and Case 6)

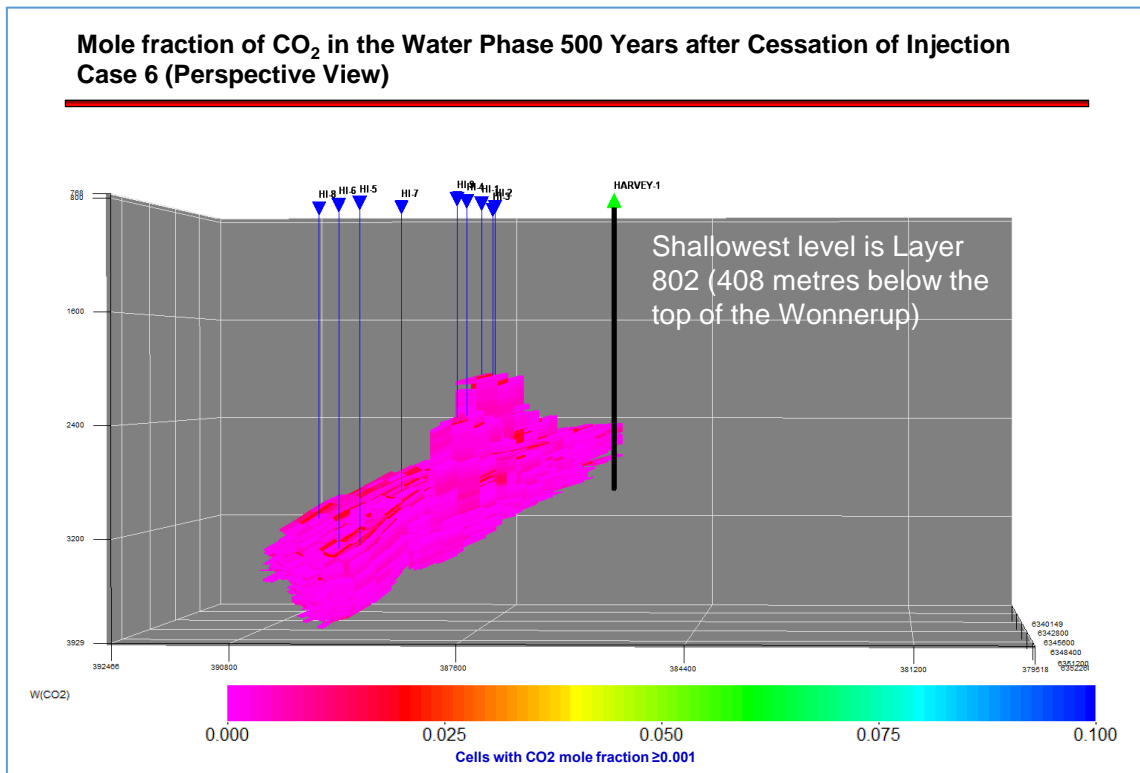


Figure 53 X-Section View – CO<sub>2</sub> Distribution (Case 6)

### 6.8.7 Case 7 – Faults transmissibility multiplied by 0.1

The net-to-gross ratio in the Wonnerup is close to 90% and the throws of the faults are generally modest compared to the thickness of the sands. This suggests that the faults are unlikely to be baffles or barriers to the flow of fluids. Nevertheless, cataclastic processes might result in some of the faults having lower transmissibility. To model this effect, a transmissibility multiplier of 0.1 was used on all faults to increase the resistance to flow between the cells affected by the faults to investigate if the lower lateral transmissibility would result in the injected CO<sub>2</sub> preferentially flowing vertically.

Figure 54 shows that there is essentially no difference the aerial extent of the CO<sub>2</sub> plume in the Reference Case and Case 7 with more spreading of the plume in the NW-SE axis. Figure 55 shows that the spread of the plume along the NW-SE resulted in less migration of the plume vertically.

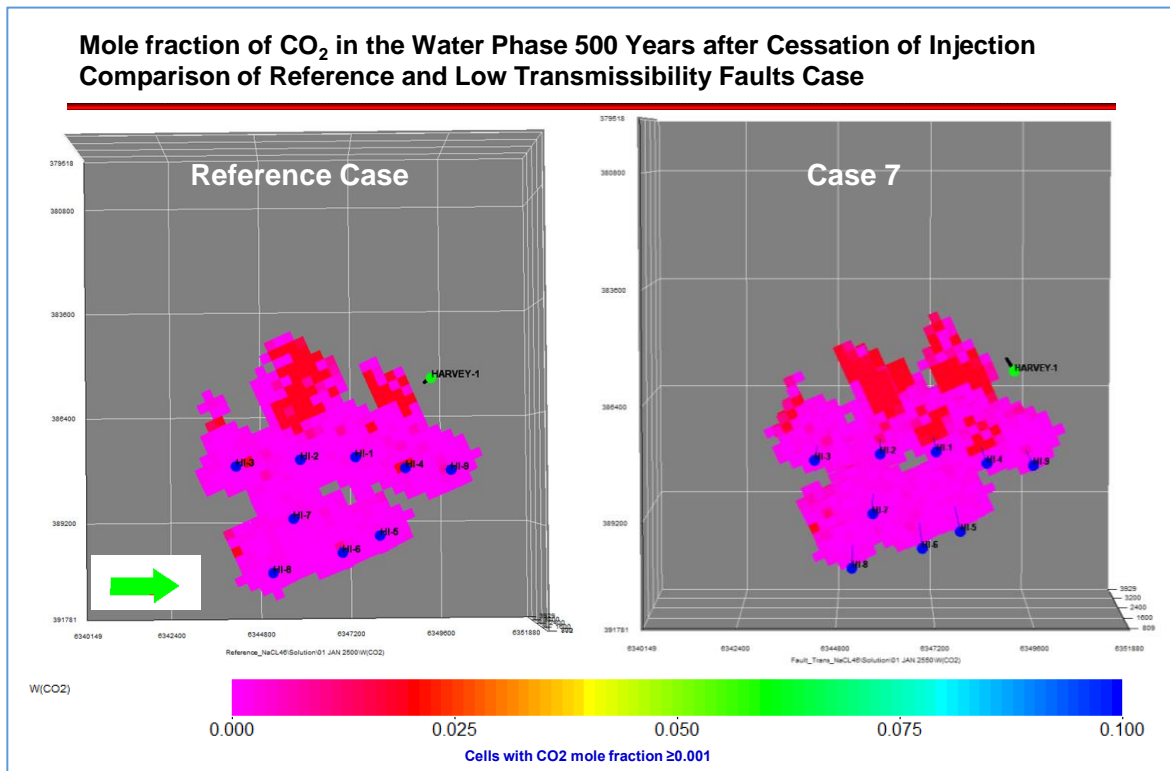
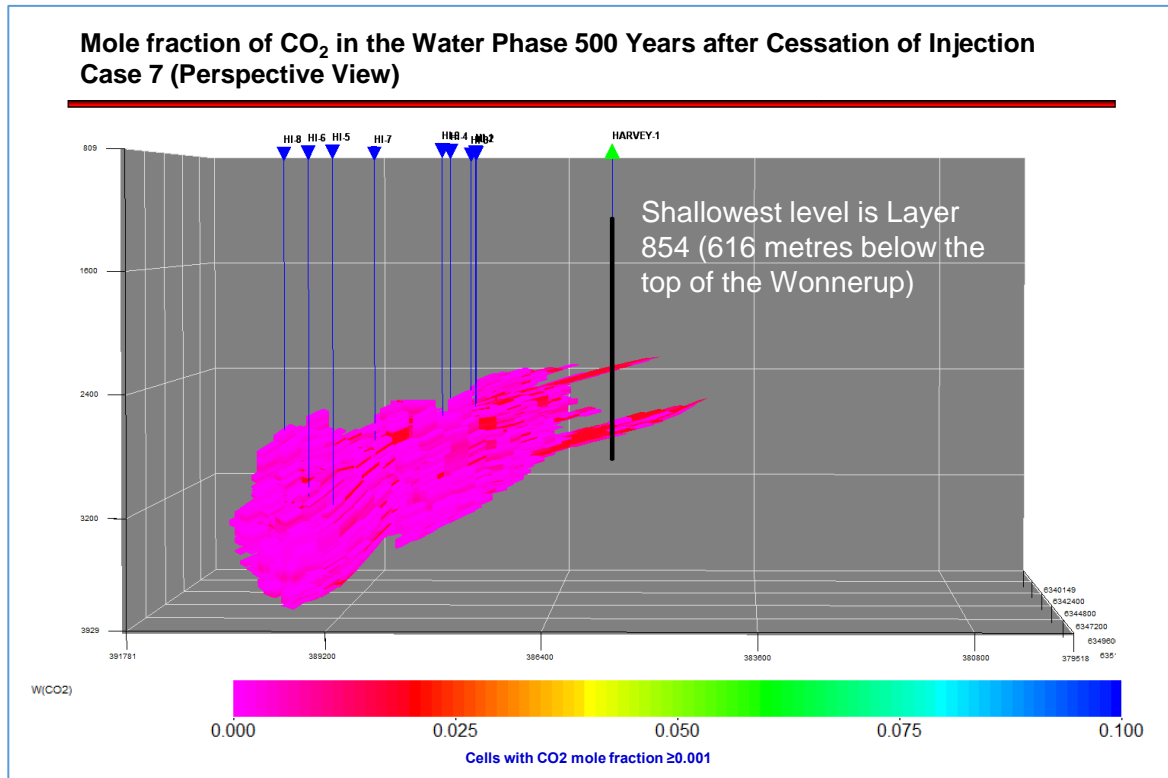


Figure 54 Top View – CO<sub>2</sub> Distribution (Comparison of Reference Case and Case 7)





**Figure 55 X-Section View – CO<sub>2</sub> Distribution (Case 7)**

### 6.8.8 Case 8 – Low CO<sub>2</sub> Solubility

The use of large grid used in the simulation of CO<sub>2</sub> injection processes can lead to uncertainty in the amount of CO<sub>2</sub> dissolved in the formation brine. During the injection stage of the storage project, the large grid blocks used in simulations resulted in an overestimate of the amount of CO<sub>2</sub> dissolved in the brine (Reference 9). To address the issue raised by Reference 9, we investigated the impact on the plume movement by reducing the solubility of CO<sub>2</sub> in brine by assuming a brine salinity of 200 g/L H<sub>2</sub>O NaCl Equivalent.

Figure 56 compares the number of moles of CO<sub>2</sub> dissolved in the brine in Case 8 and the Reference Case. The increase in the brine salinity resulted in an almost 20% reduction of CO<sub>2</sub> dissolved in the brine and an increase in the number of moles in the supercritical phase.

Figure 57 shows that decreasing the solubility of CO<sub>2</sub> in the brine has resulted in a small change in the areal extent of the plume particularly towards the NW. With less gas

dissolved in the brine, more of the CO<sub>2</sub> migrates vertically (Figure 58) and CO<sub>2</sub> is observed at a shallower depth in the model.

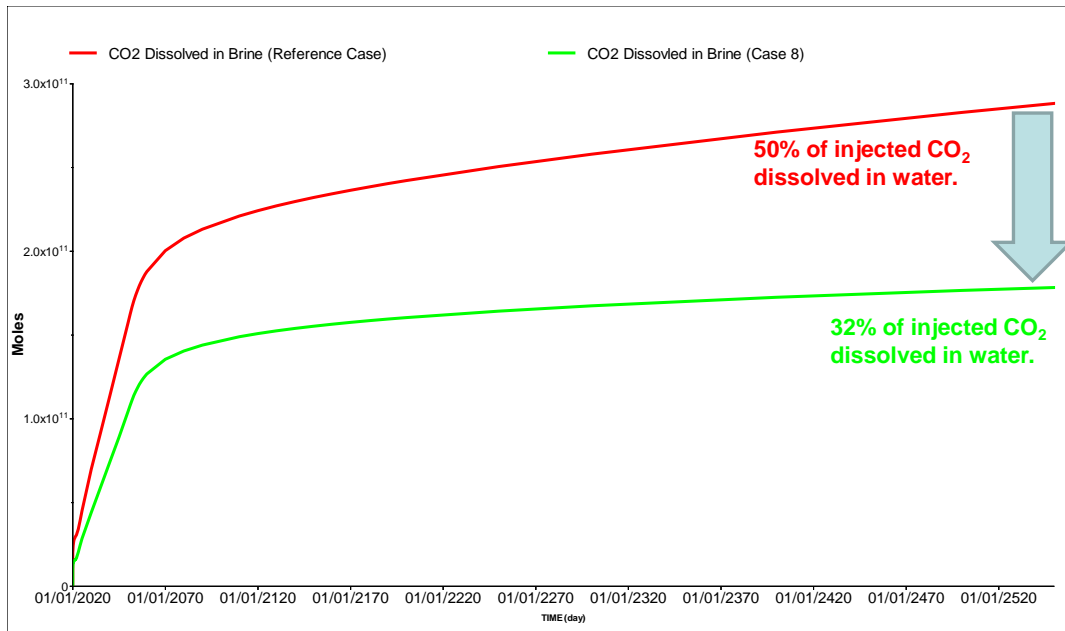


Figure 56 CO<sub>2</sub> Solubility in Brine (500 years after Cessation of Injection)

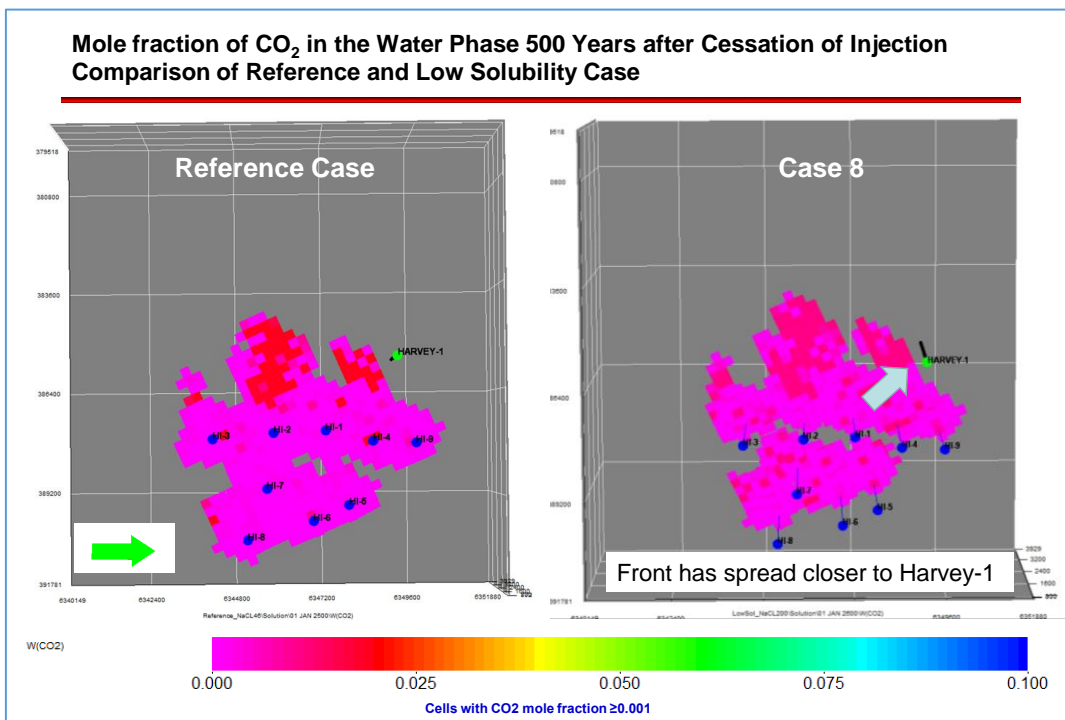


Figure 57 Top View – CO<sub>2</sub> Distribution (Comparison of Reference Case and Case 8)

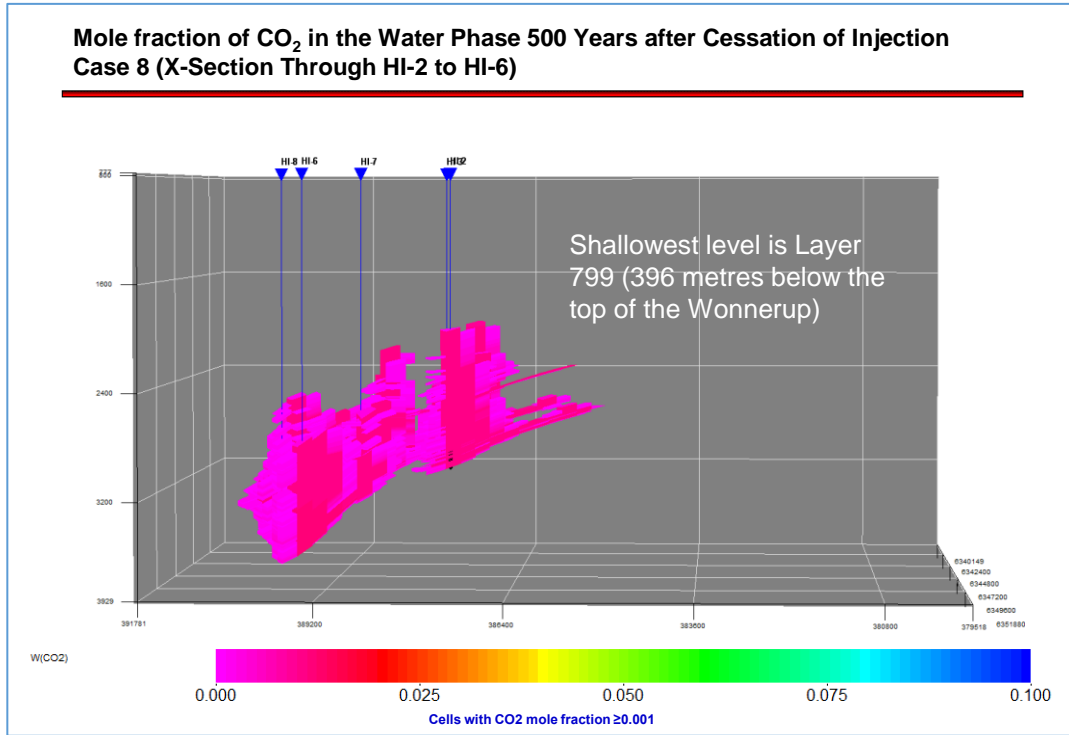


Figure 58 X-Section View – CO<sub>2</sub> Distribution (Case 8)

## 7. STRESS SCENARIOS

Two stress scenarios examining the impact of “extreme” assumptions on the migration of the CO<sub>2</sub> plume in the Harvey area were investigated.

- 1) Case 9 (High Rate) - this case assumes that the mass of CO<sub>2</sub> injected is significantly higher. The parameters of the run are:
  - Injection of 3 million tpa of CO<sub>2</sub>.
  - Reference Case model
  
- 2) Case 10 (Low trapped gas saturation and low solubility) - this case combines the assumption of low trapped gas saturation and low solubility to increase the amount of CO<sub>2</sub> available to migrate vertically. The parameters of the run are as follows:
  - Trapped gas saturation is assumed to be 10%
  - Salinity of the water is 200 g/L H<sub>2</sub>O NaCl Equivalent.
  - Injection of 800,000 tpa of CO<sub>2</sub>.

Table 9 is a summary of the assumptions and parameters of the cases.

Case	Model Name	Geological Model	Trapped Gas Saturation	Brine Salinity (g/L NaCl)	Internal Faults	End Point Gas Relative Permeability	Injection Rate (tpa)
9	HighRate	Reference	0.19	45600	Not sealing	0.12	3,000,000
10	LoHystSol	Reference	0.10	200000	Not sealing	0.12	800,00

**Table 9 Summary Table for Stress Scenarios**

### 7.1 Case 9 - High Rate

Figure 59 shows that 3 million tonnes per annum of CO<sub>2</sub> could be injected into the Wonnerup and up to 90 million tonnes could be sequestered over 30 years. The slight drop in injectivity in the early years dissipates quickly as the mobility of the fluid around the well decreases due to high CO<sub>2</sub> saturation. The bottom hole pressure profiles of the injectors (Figure 60) show that displacing the low mobility water phase results in increasing bottom hole pressures until the constraint is reached. Shortly thereafter, injectivity improves as the mobility of the fluids in the near well bore region reduces due to the increase in CO<sub>2</sub> saturation.

Figure 61 shows that, as expected, the increased mass of CO<sub>2</sub> injected results in an increase in the areal extent of the CO<sub>2</sub> plume with the plume almost reaching Harvey-1. The increase injection results in the CO<sub>2</sub> plume rising to just below the top Wonnerup (Figure 62). It should be noted that all of the CO<sub>2</sub> is contained within the Wonnerup despite the mass of gas injected was increased by more than 300%

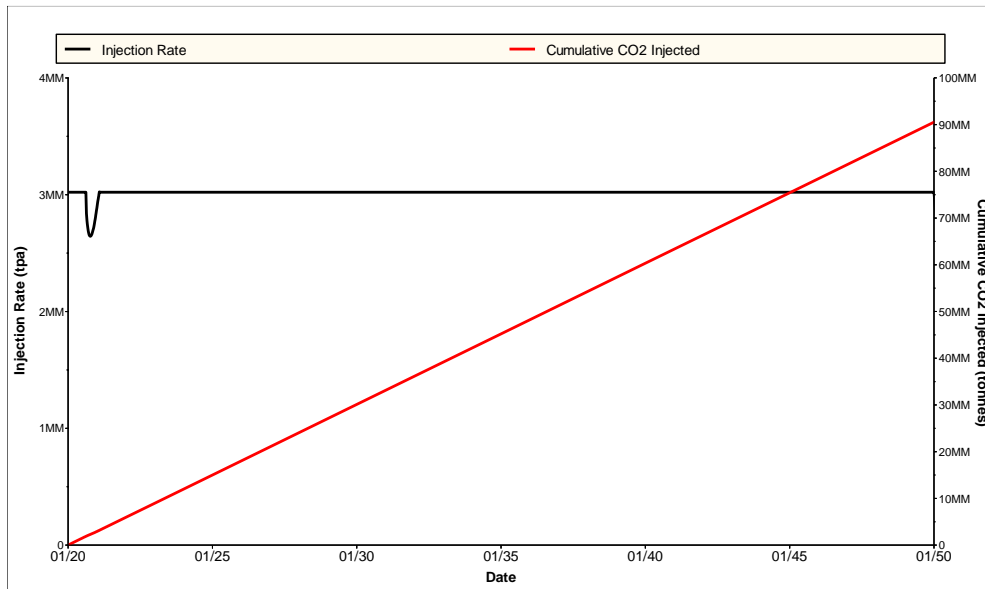


Figure 59 Injection Performance –Case 9

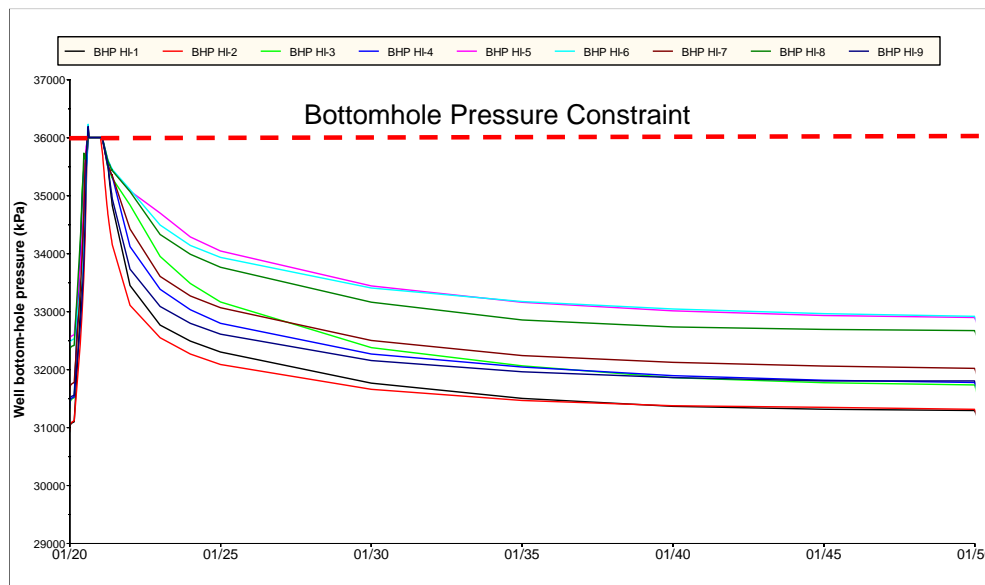


Figure 60 Bottom Hole Pressure Profile by Well During Injection – High Rate Case

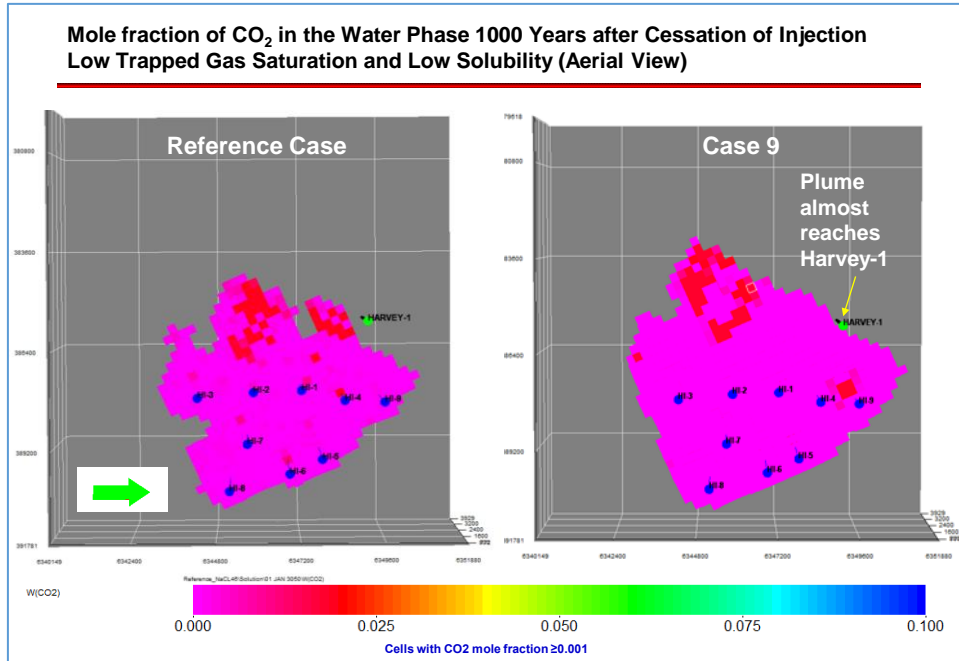


Figure 61 Top View - CO<sub>2</sub> Distribution (Reference Case and Case 9)

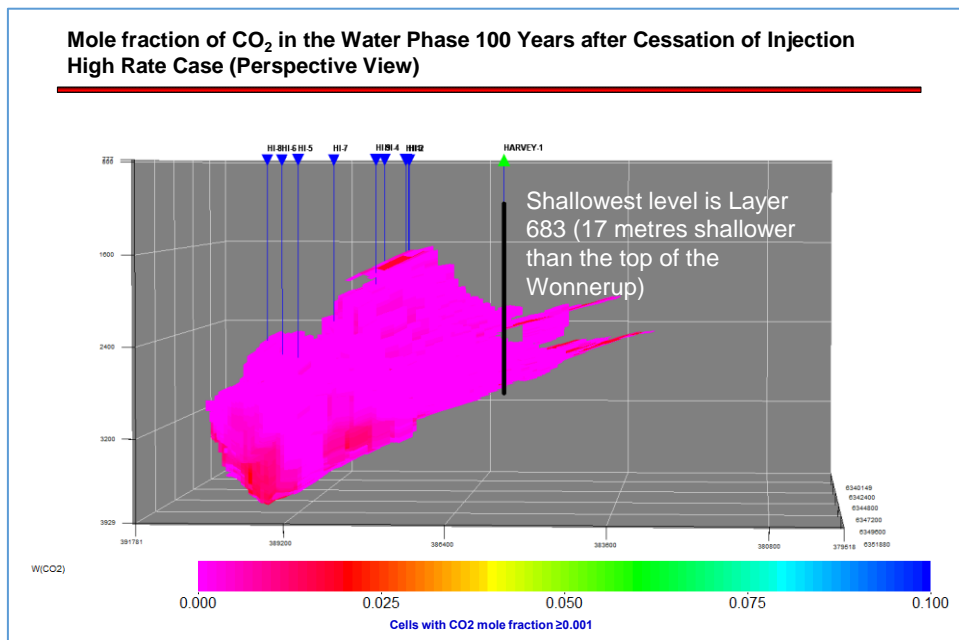


Figure 62 X-Section View – CO<sub>2</sub> Distribution (Case 9)

## 7.2 Case 10 – Low Solubility and Low Trapped Gas Saturation

This scenario investigates the impact of low solubility and low trapped gas saturation on the migration of CO<sub>2</sub> in the Wonneurup. Figure 63 shows that the decrease in both these

parameters results in the plume migrating towards the SW (i.e. shallower) but the plume is still contained in the Wonnerup (Figure 64).

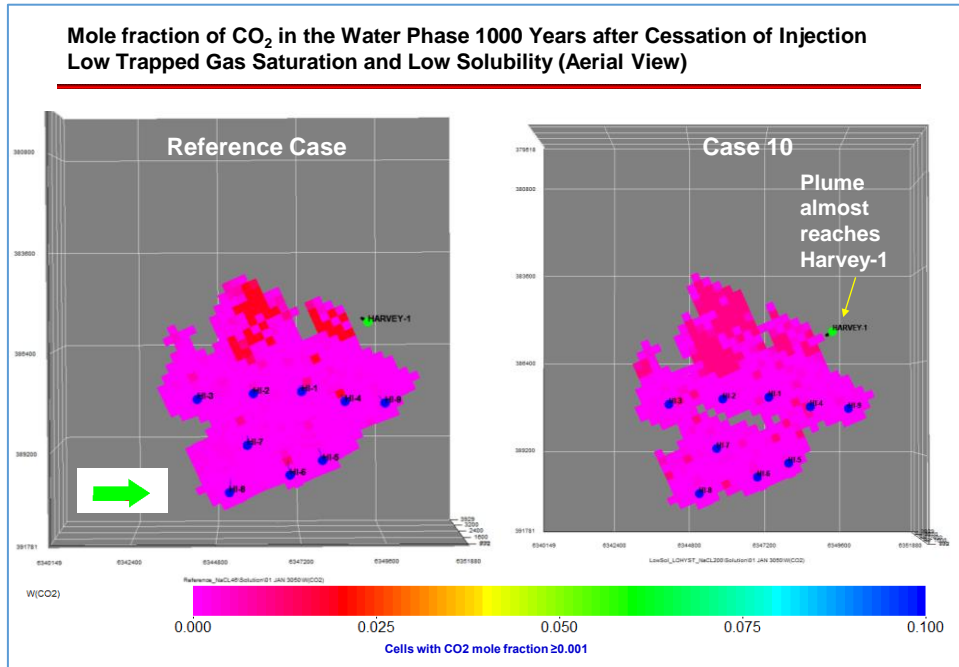


Figure 63 Top View - CO<sub>2</sub> Distribution (Reference Case and Case 10)

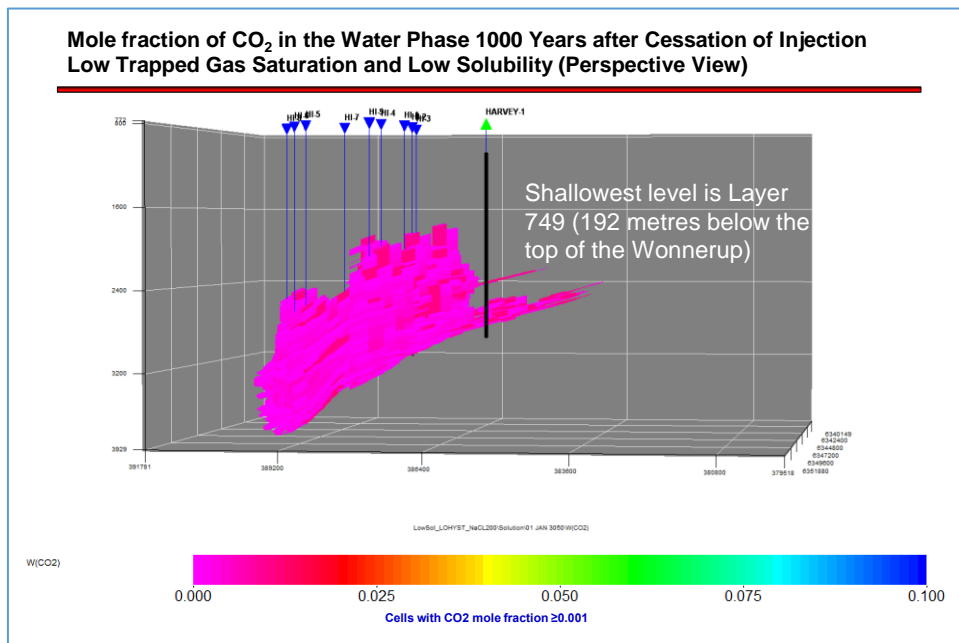


Figure 64 X-Section View – CO<sub>2</sub> Distribution (Case 10)

## 8. FURTHER WORK

---

The results of the modelling show that it could be feasible to inject 800,000 tpa of CO<sub>2</sub> over 30 years in the Yalgorup and Wonnerup formations in the Harvey area. Our modelling studies show that all of the injected CO<sub>2</sub> remains in the Wonnerup and that the main factors controlling CO<sub>2</sub> plume migration are trapped gas saturation and the solubility of CO<sub>2</sub> in brine. Uncertainties in end point relative permeability, vertical permeability or the fraction of high energy facies in the Wonnerup are a second order effect. The study also highlights the paucity of SCAL and water salinity data from the Harvey area which can be used to further constrain the range of results from the simulation studies.

It is recommended that more SCAL data be obtained from the Harvey area. More data is required in the following areas:

- Steady state trapped gas saturation for High and Low Energy Facies.
- Supercritical CO<sub>2</sub> – water capillary pressure curves at reservoir conditions for High and Low Energy facies.
- Solubility and geochemical reaction data for CO<sub>2</sub> and the formation brine.

ODIN also recommends that detailed fine grid simulations be conducted to examine the impact of coarsening the grid in the lateral direction and also to calibrate the solubility of CO<sub>2</sub> in the coarse grid blocks.



## 9. REFERENCES

---

1. Delle Piane, C., Olierook, H.K.H., Timms, N.E., Saeedi, A., Esteban, L., Rezaee, R., Mikhaltsevitch, V., Lebedev, Maxim. 2013. *"Facies-based rock properties distribution along the Harvey 1 stratigraphic well."* CSIRO Report Number EP133710
2. Core Laboratories Petroleum Services Division. *"Advanced Core Analysis Study Department of Mines and Petroleum Harvey 3."* HOU-150878
3. *Personal Communication*, Louise Stelfox and David Lim, May 2016
4. Core Laboratories Australia. *"Water Analysis Report for DMP Harvey-4."* AFL 2015018
5. Rockwater. *"Harvey 3 Lesueur Formation Fluid Sampling"*, August 2015
6. Castillo, D. *"Geomechanical Assessment of the Harvey Area."* ODIN Reservoir Consultants, DMP/2015/2
7. Zhan, Y.: *"2D Seismic Interpretation of the Harvey Area, Southern Perth Basin, Western Australia"* GSWA Record 2014/7
8. Strachan, G. *"Static Model of the Harvey Area"*, ODIN Reservoir Consultants, DMP/2016/4
9. Christopher O. Green and Jonathan Ennis-King. *"Convective mixing in geological storage of CO<sub>2</sub>."*, CSIRO Report Number EP13096, February 2013